

# The relation between cobble revetments, sand and overtopping

A numerical approach with OpenFOAM ®

Piet Zaalberg

May 7, 2019





# The relation between cobble revetments, sand and overtopping

A numerical approach with OpenFOAM ®

**Piet Zaalberg**

In partial fulfilment of the requirements for the degree of  
Master of science  
in Civil Engineering  
at the Delft University of Technology  
to be defended publicly on Thursday 16 May at 4:00 PM

## **Thesis committee**

Prof.dr.ir S.G.J. Aarninkhof  
Dr.ir. B.Hofland  
Dr.ir. A.Antonini  
Ir. W.Ockeloen

Delft University of Technology  
Faculty Civil Engineering and Geosciences  
Department of Hydraulic Engineering  
Section of Coastal Engineering  
May 7, 2019





# Acknowledgements

Thank you mom and dad for your unconditional support. Forever interested, encouraging and enthusiastic. Always keen to know what I am doing and how I am proceeding.

I am grateful to my brothers Dick, Bas and Joost, whom I'm most proud of, every single day!

I would like to thank Wouter Ockeloen for your positive attitude, your patience, the chitchats, and accurate feedback.

My gratitude goes out to Van Oord: Greg Smith, Arthur Zoon, Teun Jager and Dennis van Kesteren. It was fantastic to have the opportunity to work the majority of my research in your facilities. What a cracking place to work!

I would like to express my gratitude for the members of my committee at the TU Delft: Prof. Stefan Aarninkhof for your enthusiasm from the very first phone call and insights along the way. Dr. Bas Hofland for your unstoppable stream of ideas and knowledge. Dr. Alexandro Antonini for your help with OpenFOAM and experience.

Last but by no means least, I want to thank my ever-lasting cheerleader, my love and never-ending source of technical insights: Gijsje!

Den Haag, May 7, 2019



# Abstract

A novel type of coastal defence structure has been built on the Maasvlakte II: a dynamic cobble revetment. However, during recent years sand has washed-in between the cobbles altering its hydrodynamic performance. The central research question in this dissertation was: What is the influence of a decrease in porosity and cobble layer thickness on the overtopping as a result of sand washing-in to a cobble revetment?

As physical experiments need to be conducted on a scale large enough to prevent Reynolds scale effects, it was financially and practically unfeasible for this work to undertake such effort. Through a literature study the (dis)advantages of the existing numerical models capable of solving the Navier-Stokes equations have been reviewed. OpenFOAM with the waves2foam toolbox was identified as the most suitable numerical model for simulating overtopping on a cobble revetment, as it is depth resolving, capable of modelling flow in porous media, and it can generate and absorb irregular waves.

A data set has been obtained for the validation for the results of the OpenFOAM model, it features the physical experiments conducted in the Delta Flume completed during the design phase of the Maasvlakte II revetment scaled by 1:5. This data set contained: test S1T4 and the S2T4. In the S1 experiment series no sand was washed-in the cobble layer, in the S2 experiment 50% of the cobble layer thickness had been washed-in with sand. In the experiments the cobble layer had been exposed to irregular waves and overtopping occurred in both experiments.

The numerical wave flume has been setup and a thorough mesh study has been conducted in the process. As the cobbles cannot move in the numerical model, the numerical overtopping discharges are obtained by averaging the results of the simulations using the cross shore profile measured at the start and a profile measured the end of the S1T4 and S2T4 test. The specific overtopping discharge for the cobble layer on top of an impermeable sand core is estimated within 26% error for a cobble layer without sand washed-in to its profile (S1T4 test), and within an error of 1% for a cobble layer that is washed-in with sand (S2T4 test).

The dynamic behaviour of the cobbles during the physical tests is cumbersome to approximate in the static numerical profile and remains the largest source of uncertainty in the validation as can be seen by the numerical experiments aiming to reproduce the S1T4 experiment. The spatial and temporal changes of the KC number, median cobble diameter and porosity are not captured in the simulations and remain an other source of uncertainty. These parameters are related to the simplification of the characteristics of the porous medium. This is, however, inherently connected to the application of the Darcy-Forcheimer equation in the Navier-Stokes equation. Other sensitivities of the model have been explored as well, such as the effect of seed selection and the influence of the resistance coefficients for the Darcy-Forcheimer equation. These effects were not substantial.

The process of washing-in of sand in the cobble layer is simplified to two dominant processes: (i) change in porosity, and (ii) reduction of the effective cobble layer thickness of the S2T4 profile and of a composite slope. 16 simulations have been completed to quantify its maximum influence.

Both a decrease in porosity, and a decrease in cobble layer thickness lead to a reduction of pore volume in the cobble layer, and as a result, an increase in overtopping discharge. But how much, what is the relation?

The idea is that a part of the volume of the overtopping wave run-up tongue is sinking into the pores of the cobble revetment and does not overtop. This is a somewhat similar approach as Steeg, Breteler, and Provoost 2016 used. This theory can be captured in a new dimensionless number which accounts for the total volume of pores between the cobbles above the mean waterline called the relative pore volume number:

$$\frac{n_p \cdot R_c \cdot \sqrt{1 + \cot^2 \alpha} \cdot T_c}{H_{m0}^2}$$

In which  $n_p$  is the porosity,  $R_c$  the crest height,  $\alpha$  the slope of the revetment above the waterline,  $T_c$  the effective thickness of the cobble layer above the water line and  $H_{m0}$  the spectral wave height.

When the relative pore volume number is set out against the relative overtopping rate,  $q / (g H_{m0}^3)^{1/2}$ , it shows a clear logarithmic correlation for the parameter space covered in this research. The larger the relative pore volume number, the smaller the relative overtopping rate.

The volume of pores above the mean water level is thus correlated to a reduction in overtopping. The influence factor for roughness of the general formula for predicting the mean overtopping discharge on a slope (EurOtop 2018) is modified by comparing a fit through the reference curve of all the numerical and physical experiments. A regression through these points make that the roughness factor can now be calculated as a function of the relative pore volume per area with the following formula:

$$\gamma_f = 0.77 - 0.46 \cdot \frac{n_p \cdot T_c}{H_{m0}}$$

for

$$0.21 \leq \frac{n_p \cdot T_c}{H_{m0}} \leq 2.77 \quad \text{and} \quad T_c \leq L_{infiltration}$$

However, when using this relation one must be cautious, the EurOtop 2018 formula for overtopping (equation 5.6) on gentle slopes is sensitive to the breaker parameter,  $\xi_{m-1,0}$ .

Also, the cobble diameter has been determined according to the stability number scaling law, which is linear. The infiltration rate, however, does not scale linearly with the median cobble diameter. This scaling effect means that with the model scale results the infiltration rate on prototype scale will be underestimated and the overtopping rate, thus, overestimated.



# Contents

<b>1</b>	<b>Introduction</b>	<b>13</b>
1.1	Context and background . . . . .	13
1.2	Research question . . . . .	14
1.3	Approach . . . . .	14
1.4	Methodology . . . . .	15
1.5	Thesis outline . . . . .	19
<b>2</b>	<b>Literature Review</b>	<b>20</b>
2.1	Irregular wave run-up . . . . .	20
2.2	Irregular wave overtopping . . . . .	20
2.3	Cobble revetments exposed to irregular waves . . . . .	21
2.4	Numerical models . . . . .	22
2.4.1	Flavours . . . . .	22
2.4.2	Strengths and limitations . . . . .	23
2.5	Conclusions . . . . .	24
<b>3</b>	<b>Laboratory Experiments</b>	<b>27</b>
3.1	Context . . . . .	27
3.2	Experimental procedures . . . . .	28
3.3	Criteria for the experimental data for numerical validation . . . . .	28
3.4	Experimental data . . . . .	29
3.4.1	Profile asymmetry . . . . .	30
<b>4</b>	<b>Numerical experiments</b>	<b>31</b>
4.1	OpenFOAM, Waves2Foam and OceanWave3D . . . . .	31
4.2	Numerical model . . . . .	31
4.2.1	Navier-Stokes equations . . . . .	32
4.2.2	Turbulence and resistance parameters . . . . .	32
4.2.3	Tracking of the free surface . . . . .	33
4.2.4	Generation of free surface waves . . . . .	33
4.2.5	Measuring overtopping . . . . .	33
4.3	Setup for the simulations . . . . .	34
4.3.1	Domain . . . . .	34
4.3.2	Revetment . . . . .	34
4.3.3	Time step . . . . .	35
4.3.4	Boundary conditions . . . . .	35
4.4	Mesh study . . . . .	35
4.4.1	Conclusion . . . . .	36
4.5	Validation with respect to the overtopping . . . . .	36

4.5.1	Wave conditions . . . . .	36
4.5.2	Numerical representation of the revetment . . . . .	38
4.5.3	Overtopping comparison . . . . .	40
4.6	Sensitivity analysis . . . . .	41
4.6.1	Seed for pseudo-random wave generator . . . . .	41
4.6.2	Sensitivity in resistance coefficients of the Darcy-Forcheimer equation . . . . .	42
4.7	Variation in sand content in cobble layer . . . . .	43
4.7.1	Description of the process of washing-in of sand . . . . .	43
4.7.2	Variation in porosity of cobble layer . . . . .	44
4.7.3	Variation in sand level . . . . .	44
<b>5</b>	<b>Analysis</b>	<b>48</b>
5.1	Overtopping validation . . . . .	48
5.1.1	Profile . . . . .	48
5.1.2	Performance of reproduction of S1T4 experiment . . . . .	49
5.1.3	Performance of reproduction of the S2T4 experiment . . . . .	49
5.1.4	Numerical error . . . . .	49
5.1.5	Conclusion . . . . .	50
5.2	Sensitivity analysis . . . . .	50
5.2.1	Seed for pseudo-random wave generator . . . . .	50
5.2.2	Sensitivity in resistance coefficients . . . . .	50
5.3	Variation in sand content in cobble layer . . . . .	51
5.3.1	Variation in porosity . . . . .	51
5.3.2	Variation in sand level . . . . .	51
5.4	Dimensionless relations of the results . . . . .	53
5.4.1	Dimensionless relation . . . . .	53
5.4.2	EurOtop (2018) . . . . .	56
<b>6</b>	<b>Discussion</b>	<b>59</b>
6.1	Infiltration depth and scaling . . . . .	59
6.2	Profile shape . . . . .	61
6.3	Turbulence . . . . .	62
<b>7</b>	<b>Conclusions</b>	<b>63</b>
7.1	Sub-questions . . . . .	63
7.2	Research question . . . . .	64
<b>8</b>	<b>Recommendations</b>	<b>67</b>
<b>A</b>	<b>Site visit</b>	<b>69</b>
A.1	Introduction . . . . .	69
A.2	Observations . . . . .	70
A.2.1	Cross shore mark 3250m . . . . .	70
A.2.2	Cross shore mark 2950m . . . . .	70
A.2.3	Cross shore mark 2850m . . . . .	74
A.3	Concluding remarks . . . . .	75

<b>B Mesh Study</b>	<b>76</b>
B.1 The design . . . . .	76
B.2 Wave propagation . . . . .	77
B.3 Wave run-up and overtopping . . . . .	78
B.4 Conclusion . . . . .	81
<b>Bibliography</b>	<b>82</b>

# List of Figures

1.1	Methodology used in the work presented. . . . .	18
3.1	Plan of Delta flume at Marknesse. . . . .	27
3.2	Overview of the physical model test wave conditions on prototype scale. . . . .	28
3.3	Overview of the average cross shore profiles after each of the wave conditions during S2 experiments (prototype dimensions). . . . .	29
3.4	Asymmetrical profile development during the S1 test series. . . . .	30
4.1	Overview of the numerical grid in Paraview. Note the non-equidistant grid-sizes, the relaxation zone inlet in white and the relaxation zone outlet in red. . . . .	34
4.2	Cross shore profile of the numerical setup. The sand is hydraulically impermeable, the median cobble diameter $D_{n,50} = 0.015m$ . The numerical wave gauges are shown in this plot. . . . .	37
4.3	A comparison of the energy density spectra of the numerical and experimental tests. . . . .	37
4.4	An overview of the cross shore profiles as measured by Deltares. Note the decrease in thickness of the effective cobble layer for the S2 profiles . . . . .	38
4.5	Note that in both S1 and S2 test series the profile becomes steeper, the cobble layer of the revetment thinner and the crest is slightly elevated. . . . .	39
4.6	Overview of the numerical grid in Paraview with the sand slope cut out of the domain. Also note the finer meshes in and around the cobbles. . . . .	39
4.7	Cumulative overtopping comparison of the numerical experiments and the data provided by Deltares. . . . .	40
4.8	A total of 6 simulations reproducing the S2T4 experiment in which only the seed number for the random wave generator varies. . . . .	42
4.9	Overview of the sand levels within the cobble layer for each of the simulations. . . . .	45
4.10	An overview and detail of the composite slope consisting of a 1:9 and 1:4 slope. . . . .	46
5.1	The relation between the dimensionless overtopping rate and dimensionless relative cobble layer thickness and median cobble diameter. . . . .	53
5.2	For both figures great correlation is observed. However, in figure 5.2a some degree of scatter is observed around $n_p \cdot T_c / H_{m0} \approx 2$ as the influence of the crest height misses. . . . .	54
5.3	The relation between dimensionless pore volume number is set out against the relative overtopping rate for the results of the numerical experiments, as well as the physical experiments. . . . .	55
5.4	The relation between the relative pore volume per area and roughness factor. . . . .	57

6.1	The relation between the flow resistance in the porous medium approximated by Darcy-Forcheimer and cobble diameter size for porosity $n_p = 0.30$ and $n_p = 0.40$ . . . . .	60
A.2	Bottom of the revetment at cross shore mark 3250m . . . . .	70
A.3	Middle of the revetment at cross shore mark 3250m . . . . .	71
A.4	Top of the revetment at cross shore mark 3250m . . . . .	71
A.5	Bottom of the revetment at cross shore mark 2950m . . . . .	72
A.6	Bottom of the revetment looking into northerly, respectively southerly direction at cross shore mark 2950m . . . . .	72
A.7	Middle of the revetment at cross shore mark 2950m . . . . .	72
A.8	Middle of the revetment looking into southerly direction at cross shore mark 2950m . . . . .	73
A.9	Top of the revetment at cross shore mark 2950m . . . . .	73
A.10	Bottom of the revetment at cross shore mark 2850m . . . . .	74
A.11	Middle of the revetment at cross shore mark 2850m . . . . .	74
A.12	Top of the revetment at cross shore mark 2850m . . . . .	75
B.1	A screen grab of the refinement on the top of the revetment and the sand core. This refinement enables measurements of the relatively thin layer of water that exist during overtopping events. . . . .	77
B.2	Surface elevation over time measurements of wave gauge 2 at $x = 124.5m$ and wave gauge 4 at $x=150$ m. . . . .	79
B.3	Cumulative overtopping over time measurements for 4 simulations with different mesh resolutions. The mesh with the lowest resolution is not able to capture the overtopping events properly. Case GB08 with 11328 active cells does capture the overtopping lens, however poorly. Cases with an increased resolution GB01 and GB03 capture the processes well and converge. . . . .	80
B.4	A visual comparison of the same wave breaking event calculated by two different mesh resolutions. . . . .	81

# List of Tables

2.1	A summary of the most relevant formulae predicting run-up resulting from irregular waves on smooth impermeable slopes (Arana, 2017)	25
2.2	An overview of the most relevant formulae predicting overtopping resulting from irregular waves	26
3.1	A summation of the target conditions and measured results from test S1T4 and S2T4 on model scale. The specific discharge $q$ is calculated based on total overtopping volume divided by the time and the width of 1m the asymmetrical west part of the revetment where most of all the overtopping occurred.	30
4.1	Overview of the inputs used for the mesh study and validation of the simulations.	35
4.2	Overview of the two meshes used for the numerical simulations and their dimensionless characteristics.	36
4.3	The average specific discharge data from the experiments S1T4 and S2T4 are compared to the numerical simulations in OpenFOAM. A total of four simulations were conducted: two with the profile SxT3 profile and two with the SxT4 profile.	41
4.4	The two most commonly used resistance closure coefficients for flow in porous breakwaters and coastal structures as a result of waves (Inigo J Losada et al. 2016).	42
4.5	The results of simulations in which the porosity is varied between the minimum and maximum values of those measured in the physical experiments. Both the cross shore profile of the S1T4 and the S2T4 experiments have been simulated.	44
4.6	The results of simulations in which the sand level in the cobble layer is varied. The cobble layer thickness is reduced by raising the internal sand level. The cross shore profile of the S2T4 experiment has been used.	45
4.7	The results of simulations in which the thickness of the cobble layer is varied. The cobble layer thickness is reduced by decreasing the cobble height and keeping the cobble-sand interface in the same position. A composite slope consisting of two straight slopes has been used. Furthermore, in five simulations the median cobble diameter was $D_{n,50} = 15mm$ and in four simulations $D_{n,50} = 152mm$	47
5.1	Comparison of the parameter range of the study of Steeg, Breteler, and Provoost 2016 into the effect of porosity on the influence factor $\gamma_f$ of equation 5.6 and the numerical experiments conducted by Zaalberg 2019 and the experiments conducted in the Delta Flume 2007.	56

B.1	Overview of the several mesh resolutions and their dimensionless characteristics. . . . .	77
B.2	A multi criteria assessment of the quality of the mesh for the wave propagation zone, i.e. the zone from the start of the domain at $x = 104m$ until the zone of were wave breaking almost occurs at $x = 150m$ . . . . .	78
B.3	A multi criteria assessment of the quality of the meshes for physical processes of run up and overtopping. A much higher mesh resolution is required to model these processes of interest correctly, i.e. the steep and overturning waves, the thin water layer during overtopping and flow in the porous cobble layer. . . . .	80

# List of Symbols

Wave parameters	$c$	$[m]$	wave celerity
	$f$	$[m]$	frequency
	$H_0$	$[m]$	deep water wave height
	$H_{m0}$	$[m]$	$H_{m0} = 4(m_0)^{1/2}$ - spectral wave height
	$k$	$[m^{-1}]$	wave number
	$L$	$[m]$	wave length
	$L_0$	$[m]$	$T_{m-1,0} = gT_{m-1,0}^2/2\pi$ - deep water wave length
	$L_{m-1,0}$	$[m]$	$gT_{m-1,0}^2/2\pi$ - spectral wave length in deep water
	$m_n$	$[m^2/s^n]$	$\int_{f_1}^{f_2} f^n S(f) df$ - n-th moment of spectral density
	$q$	$[m^3/m/s]$	overtopping discharge per meter width
	$T_p$	$[s]$	spectral peak wave period
	$T_{m-1,0}$	$[s]$	$m_1/m_0$ - spectral wave period
	Structural parameters	$u$	$[m/s]$
$V$		$[m^3/m]$	overtopping volume per meter width
$\alpha$		$[rad]$	slope angle
$n_p$		$[-]$	porosity of porous revetment layer
$K$		$[m^2]$	permeability of porous revetment layer
$R_c$		$[m]$	crest height
Fluid parameters	$T_c$	$[m]$	effective thickness of porous revetment layer
	$\gamma_f$	$[-]$	influence factor accounting for roughness
	$\rho$	$[kg/m^3]$	fluid density
	$\sigma$	$[J/m^2]$	surface tension
	$\mu$	$[m^2/s]$	dynamic viscosity
	$\eta$	$[m^2/s]$	kinematic viscosity
	$g$	$[m/s^2]$	gravitational acceleration
Dimensionless quantities	$h$	$[m]$	water depth
	$\xi$	$[-]$	$\tan(\alpha)/\sqrt{H/L}$ - Iribarren number
	$\xi_{m-1,0}$	$[-]$	$\tan(\alpha)/\sqrt{H_{m0}/L_{m-1,0}}$
	$Fr$	$[-]$	$u/\sqrt{gh}$ - Froude number
	$KC$	$[-]$	$u \cdot T/L$ - Keulegan-Carpenter number

# Chapter 1

## Introduction

### 1.1 Context and background

Flood risks are anticipated to increase driven by the projected increases of sea surface levels, wind speeds and rainfall. Understanding changes in flood risks from waves overtopping seawalls or other structures is a key requirement for effective management of coastal defences.

On the northwestern part of the Maasvlakte II conditions are changing. The innovative dynamic cobble shore with a foreshore reef of reused concrete blocks of 3,5-kilometer long is constructed as part of the 11-kilometer long sea defence. It consists of a dynamic shore revetment, being a thick layer of crushed cobbles over a sand core with typical beach-dune profile. During the last 6 years sand is transported by wind and water and has filled a large portion of the pores of the crushed cobble layer. It has been shown by Mann 2019 that this process will continue in the foreseeable future. The sand alters the interaction between the water and cobble revetment. Despite recent interest in this field, the hydraulic behaviour of the water on a cobble revetment is still very much unclear. This is a major concern for the contractor PUMA and the Port of Rotterdam authority.

During the design phase many physical model tests have been conducted looking into the stability and cross shore transport balance of the cobble layer, but less so on the influence of sand completely filling the pores of the cobble revetment. Since hardly any experience exist for this novel revetment type - let alone its interaction with sand - trustworthy design rules and relations are yet to be developed. This work aims to fill that knowledge gap.

Detailed numerical modelling based on Navier-Stokes equations is generally a widely used engineering tool. However, the detailed numerical modelling of the free-surface waves and their interaction with permeable structures still forms a niche. Application of the OpenFoam® package coupled with the waves2Foam toolbox for the computation of wave overtopping is interesting, as it is able to economically simulate a vast amount of scenarios in a short time span - physical model tests on large scale is a costly affair and is time consuming. Since Jacobsen et al., 2015 and Van Gent et al., 2015 have successfully applied this numerical framework to wave interaction with permeable coastal structures, the way is paved for utilisation of the model for wave breaking, run-up and overtopping on the porous cobble revetment.

The benefit of this work is that the numerical model tests are not only conducted

specifically for the Maasvlakte II case, but also on standardised revetments. This enabled the author to parameterise the model outcomes in dimensionless relations and to define a relation for the roughness factor for the EurOtop 2018 formulae for overtopping on embankments as a function of pore volume per area revetment. It is expected to be applicable to any cobble layer of (fairly) similar slope and wave conditions.

## 1.2 Research question

What is the influence of a decrease in porosity and cobble layer thickness on the overtopping as a result of sand washing-in to a cobble revetment?

### Sub-questions

The following sub-questions help to find the answer to the main research question:

- (i) What is the most suitable numerical model for simulating overtopping on a cobble revetment?
- (ii) What experiments are most suitable to reproduce and thereby validate the numerical model outcomes with?
- (iii) How well can the numerical model reproduce the experiments and what are its sensitivities?

## 1.3 Approach

The approach embodies the following tangible objectives that have to be achieved to answer the main and sub research questions successfully:

- identify the most suitable numerical model for simulating overtopping on a cobble revetment
- obtain data suitable to validate the numerical model outcomes with
  - explore relevant experiments
  - formulate relevant selection criteria
  - obtain the data from the relevant experiments
- setup and validate numerical wave flume
  - setup computationally efficient numerical grid without losing crucial information
  - generate numerical waves statistically identical to data of Deltares
  - construct representative numerical cobble shore with correct characteristics such as slope porosity, stone diameter, thickness and washed-in sand level.
  - validate correct working of model by comparing numerical overtopping discharge with measured overtopping discharge for simulations
  - perform sensitivity analysis with respect to Darcy-Forcheimer coefficients and grid resolution.

- perform sensitivity analysis with respect to different realisations of the surface elevation of the energy density spectrum.
- conduct numerical simulations to investigate the effect of the washing in of sand between the cobbles on the overtopping
  - simulate numerical scenarios with 0%, 50%, 75%, 90% and 100% of sand washed-in with respect to the thickness of the cobble layer
  - determine the effect of the porosity of the cobble layers on the amount of overtopping
- find the relation between effective cobble layer thickness, porosity, crest height and overtopping
  - define dimensionless relation between relative overtopping rate and relative pore volume
  - compare with EurOtop 2018 formulae; and if possible, formulate  $\gamma_f$  as a function of pore volume per area

## 1.4 Methodology

The methodology used in this thesis comprises of several stages and can be divided according to the five main objectives stated above. The flowchart in figure 1.1 provides a visual overview.

### Identify the most suitable numerical model

A literature study was completed to identify the most suitable numerical model capable of simulating wave propagation, wave breaking, porous flow and overtopping.

### Selection of data to validate the numerical model

Data from model tests conducted during the design and construction of the Maasvlakte 2 have been obtained. The purpose of these data sets was to validate the results of the numerical model. Unfortunately, none of the data sets had an high temporal resolution. To allow for a successful validation of the numerical model the data had to comply to the following criteria:

- overtopping had to occur in the experiment, and
- the data should include an experiment with sand washed-in to the revetment and an experiment without sand washed-in, and
- measurements of the cross shore profile of the cobbles before and after the experiments must be available.

Two experiment tests complied: experiments S1T4 and S2T4. In the S1T4 experiment no sand was washed-in before the experiment started, in the S2T4 experiment 50% of the cobble layer thickness was washed-in with sand before the revetment was being exposed to waves. The data sets consisted of:

- statistical wave parameters:

- spectral wave height
- peak period
- energy density spectrum
- water surface elevation over time of experiment S2T4 alone
- revetment characteristics:
  - cobble diameter distribution
  - sand distributions
  - porosity
  - cross-shore profile shape before and after the experiment
  - internal sand level before and after the experiment
- average overtopping discharges

No overtopping volumes, nor the velocity signal of the wave paddle over time measurements have been found and made available by Deltares.

### Setup and validation of the numerical model

The numerical model was set up according to the layout of the aforementioned experiments. A mesh study was conducted. It had special focus on correct representation of wave propagation and overtopping events, while being computationally efficient enough to enable long simulation times of 1600 s.

The wave conditions were compared in a statistical framework, as wave-to-wave analysis was not possible as the velocity signal of the paddle and overtopping volumes overtime measurements were not available. Two methods to generate numerical waves have been tested: OpenFOAM nested in the fully non-linear and dispersive free surface model OceanWave3D and the waves2foam module using the relaxation zone technique. The waves2foam module had shown to give the best reproduction of the energy density spectrum of the Deltares data. Furthermore, it proved to be more efficient.

The validation of the numerical model was done by measuring the overtopping in the numerical experiments and comparing that to the average overtopping data of experiments S1T4 and S2T4. OpenFOAM cannot model the movement of the cobbles and as a result the morphodynamics of the cobble layer during the experiments is not captured. Therefore, for each of the validation experiments two cross shore profiles of the cobble layer were used in the simulations: (a) the profile measured before the experiment, and (b) the profile measured after the experiment. The specific overtopping discharges,  $q$ , measured during the simulations were averaged with the following weighting:  $1/3 \cdot q_a$  and  $2/3 \cdot q_b$  and then compared with the Deltares data. The weighting was applied as the dynamic behaviour of the cross shore profile at the start of the experiment is larger than the at the end (M. v. Gent 2009).

### Conduct numerical simulations

The process of sand washing-in to the pores of the cobbles was simplified into two processes:

- (i) A decrease of the overall porosity of the cobble layer as sand will partly fill up and potentially clog the spaces between the cobbles over the whole thickness and width of the cobble layer altering the flow of water in it.

- (ii) As sand falls and washes down through the cobble layer it will fill the pores from the bottom up, effectively decreasing the thickness of the revetment where flow is possible.

Four numerical experiments were conducted for which the porosity of the cobble layer varied between  $0.29 \leq n_p \leq 0.41$ . Two experiments were based on the sand level and cross shore profile of the S1T4 experiment and two experiments on the S2T4 experiments. The goal was to map the bounds of the maximum influence of porosity.

Twelve numerical experiments have been completed in which the effective cobble layer thickness is changed. Of those twelve, three simulations featured the S2T4 cross shore profile. The complex cross shore profile prohibited a fair comparison and next to that made a parameterisation difficult, however, it gave valuable insight to the contractor PUMA. Nine of those twelve simulations featured an cross shore profile of an composite slope consisting of two straight sections with the effective thickness,  $T_c$ , of the cobble layer varying between  $0.09 \leq T_c \leq 0.94$  m. These experiments provided the data to derive the relationships between cobble layer thickness, porosity and overtopping.

### Find the relation between cobble layer thickness, porosity and overtopping

To find the dimensionless relations between all the numerical scenarios the dimensionless overtopping rate,  $q/\sqrt{g \cdot H_{m0}^3}$ , was plotted against the following dimensionless parameters:

$$\frac{n_p \cdot T_c}{H_{m0}} \quad \text{and} \quad \frac{T_c \cdot R_c}{H_{m0}^2}$$

The observed relationships inspired for an approach similar to what Steeg, Breteler, and Provoost 2016 used for water absorbing concrete blocks. The theory is that the total accessible pore volume of the revetment above the mean water surface level relates to a decrease in overtopping rate as a certain part of the up-rushing water is absorbed by the revetment. This relationship was observed by plotting the relative overtopping rate,  $q/\sqrt{g \cdot H_{m0}^3}$ , versus the dimensionless pore volume:

$$\frac{n_p \cdot R_c \cdot \sqrt{1 + \cot^2 \alpha} \cdot T_c}{H_{m0}^2}$$

Increasing the thickness of the cobble layer had an decreasing effect until the thickness is equal to the infiltration depth of water over a wave cycle as the permeability layer is limited.

The concluding step in this work was to provide the means to estimate the mean overtopping discharge on a sloping cobble layer revetment with the equations found in EurOtop (2018). Defining the influence factor for roughness,  $\gamma_f$ , as a function of the dimensionless pore volume per area seemed as a sound option considering the observed relationship in the previous analysis. This approach is again somewhat similar to the approach used in the work of Steeg, Breteler, and Provoost 2016 in the sense that a reduction of the overtopping volume by absorption of the revetment is quantified by modifying  $\gamma_f$ .

This relation was constructed by first calculating the influence factor,  $\gamma_f$ , for each simulation by comparing the data with the fit through the overtopping formula of EurOtop, with all influence factors equal to 1.0 except for the roughness factor. Now all the roughness factors,  $\gamma_f$ , had been obtained, these values were plotted versus the relative pore volume

per area. A regression through these points gave the simplified, but useful relation between the influence factor,  $\gamma_f$ , as a function of the relative pore volume per area,  $n_p \cdot T_c / H_{m0}$ , for the parameter space used in this work.

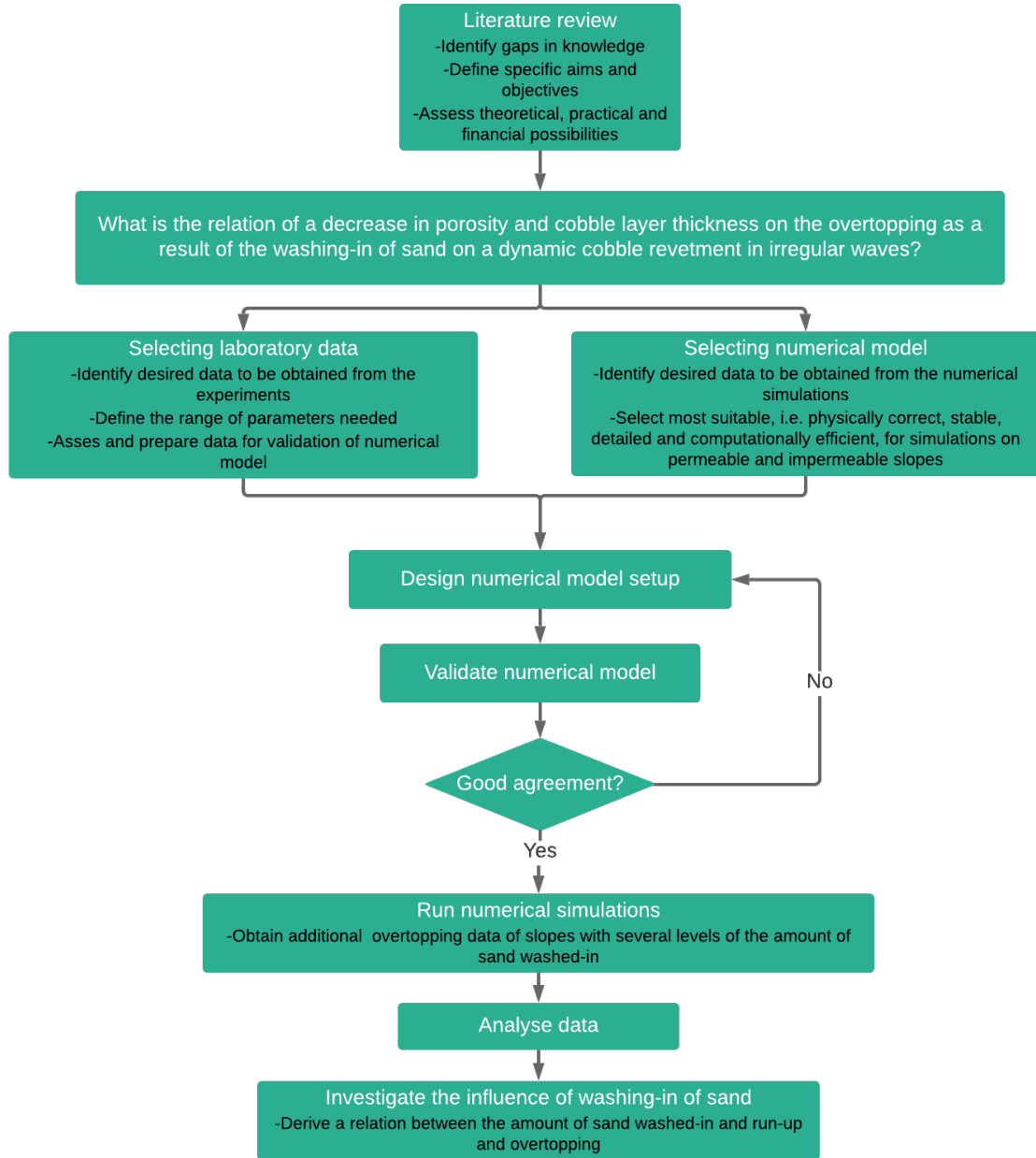


Figure 1.1: Methodology used in the work presented.

## 1.5 Thesis outline

In chapter 2 literature is reviewed. Previous work on irregular wave overtopping, cobble revetments exposed to irregular waves and type of numerical models will be explored and evaluated. Then, in chapter 3, criteria for the selection of data of physical experiments are formulated. According these criteria, the most suitable experiments are selected.

Chapter 4 describes everything regarding the numerical simulations conducted in OpenFOAM and OceanWave3D. A mesh study is conducted to find the right mesh settings, after that, the physical experiments as selected in chapter 3 are reproduced and sensitivities mapped. Now that the wave flume is validated, an extra 16 simulations are conducted to investigate the influence of sand washing-in to the cobble revetment. The results numerical experiments provide the data on which the research question will be answered.

In chapter 5 the numerical experiments are analysed. It starts with an evaluation of the numerical experiments aiming to reproduce the the physical experiments. Subsequently, the results of the sensitivity simulations are examined. Finally, for each of the 16 simulations in which porosity and sand level is varied, the results are compared with each other and an analysis of the dimensionless relations is made.

In chapter 6 the analysis and model results are put into context. Furthermore, a comparison is made with similar studies and assessed whether they extend, contradict or dispute existing knowledge. In chapter 7 the 3 sub-questions are treated, after which the conclusion with respect to the research question are made. Finally, in chapter 8, advice is given for the direction of future research.

# Chapter 2

## Literature Review

This chapter discusses previous studies and relevant literature on wave run-up, wave overtopping and the performance of cobble revetments exposed to irregular waves. It also covers studies on numerical models capable based on the Navier-Stokes equations. This chapters ends with a conclusion.

### 2.1 Irregular wave run-up

Wave height, wave length and the slope angle are the most important parameters in an idealised environment with regular normal incident waves breaking over a smooth, impermeable and plain slope. The parameters are often combined to form dimensionless parameters that in empirical or theoretical formulae attempt to predict wave run-up.

With irregular waves however, the situation is different. Not only the behaviour of a single wave on the slope must be predicted, the random behaviour of the incoming waves must be captured as well. Two main approaches exist Allsop et al., 1985. The first one being a theory based on equivalence. It entails that for irregular wave run-up, every single wave is seen as a individual, regular wave. Here, a typical run-up level for irregular waves, such as the significant run-up  $R_s$ , is determined using a run-up formula for regular waves and other run-up levels such as the  $R_{2\%}$  parameter are then estimated by the Rayleigh distribution of run-up levels.  $R_{2\%}$  is said to be representative of the wave run-up distribution of irregular wave trains is used often in formulae to predict wave run-up. The second method is based on fitting standard probability density distributions to measured random wave run-up results. The random nature of incoming waves causes each wave to have a different run-up level. Unlike regular wave run-up, which produce a single maximum value, irregular waves produce a run-up distribution.

A summary of the most relevant formulae predicting run-up resulting from irregular waves breaking on smooth, impermeable slopes is shown in table 2.1 and is based on the table as presented by Arana 2017.

### 2.2 Irregular wave overtopping

If the crest level of the dike of embankment is lower than the highest wave run-up level,  $R_{max}$ , overtopping occurs. Now, the freeboard,  $R_c$ , defined as the level difference between the still water level an the crest height, becomes an important parameter. Wave overtopping depends on the freeboard,  $R_c$ , and increases for decreasing  $R_c$ .

Calculation of mean overtopping discharge on structures is normally done using a regression model fitted to hydraulic model tests. Two formulations dominate the literature

(Andersen and Burcharth 2004):

$$Q = a \cdot \exp(-b \cdot R) \quad (2.1)$$

$$Q = a \cdot R^{-b} \quad (2.2)$$

Owen (1980) established a popular method for predicting wave overtopping in which the wave overtopping discharge,  $q$ , decreases exponentially as the crest freeboard,  $R_c$ , increases. This form of equation has become popular. It is practical as it gives a straight line on a log-linear graph, and it only has two coefficients for fitting to the data. Next to Owen, this method has also been employed by Besley 1999, Van der Meer & Janssen 1994, Pedersen 1996 and Eurotop 2007; 2018. Pedersen 1996 is excluded in the overview of table 2.2 as it is developed for crown wall rubble mound breakwaters.

### 2.3 Cobble revetments exposed to irregular waves

Until now, experiments with cobble revetments that have looked into sand washing-in the pores of the cobbles focused on its influence on profile development under wave attack (M. v. Gent 2009; Loman, Van Gent, and Markvoort 2010; López De San Román Blanco 2003; She, Horn, and Canning 2007). Observations of experiments of a dynamic cobble revetment exposed to waves scaled identical to the Maasvlakte II by M. v. Gent 2009 show that:

- most dynamic response is expected for the most permeable structure and the average slope is steepest for the most permeable structure.
- if the pores between cobbles are filled with sand the response is less dynamic and as less erosion occurs below the waterline a lower crest is expected.
- the change in profile shape is largest at the start of the experiment, and moves towards an equilibrium as the experiments continues.

Two empirical formulae exist that (can be tuned) to predict the overtopping on cobble revetments to some extent. The first one being the EurOtop 2018 formula (see table 2.2) applicable for embankments, slopes and levees. The second one is the formula for dynamically stable breakwaters, also found in EurOtop 2018, based on the experiments conducted by Sigurdarson and Van der Meer 2011.

Until this work, the general formulae to predict overtopping on over embankments, slopes and levees is not very useful for application on cobble revetments. No influence factor exists to account for the absorption of water into the pores of the cobbles. This process of infiltration of water during the run-up and run-down has been shown to be an important process when predicting wave run-up and overtopping (Arana 2017; Steeg, Breteler, and Provoost 2016). Steeg, Breteler, and Provoost 2016 found a solution to account for the lack of this influence factor. In his work he defined the influence factor for roughness,  $\gamma_f$ , as a relation of the relative porosity of the porous concrete armour. The major drawback of this relation is that the Irribarren number,  $\xi_{m-1,0}$ , has a large influence on the predicted overtopping rate. Since the prime philosophy of cobble revetments is that they are dynamic in profile, this remains a source of uncertainty.

The strength of the second formula is that it is based on experiments of reshaping breakwaters, i.e. the change in profile is intrinsically accounted for. However, for the purpose of this research this empirical formula fitted to the data of the experiments of Sigurdarson and Van der Meer 2011 is not very suitable as:

- the stability number is an order higher, resulting in a much steeper profile
- the experiments are conducted on a completely permeable breakwater
- no parameter accounting for changed in permeability or cobble layer thickness exists

The breaker parameter  $\xi_{m-1,0}$ , has large influence on wave overtopping on gentle slopes, as the breaker parameter will be quite small. The rubble mound structures reviewed in EurOtop have quite steep slopes. Due to these differences in scale of armour dimensions, geometrical parameters of the cross shore profile, and core permeability the formula for reshaping structures based on the data of the experiments conducted by Sigurdarson and Van der Meer 2011 is not applicable.

## 2.4 Numerical models

### 2.4.1 Flavours

The mathematical modelling of the interaction of water waves with porous coastal structures has continuously been among the most relevant challenges in coastal engineering research and practice. Finding a tool to better predict essential processes and how they are affected by permeability, has been hampered by computational limitations that are being overcome (Inigo J Losada et al. 2016).

Modelling multiphase fluids (water and air) when flowing through porous media is highly complex. Two flavours exist:

- (i) microscopic: each of the elements that form the material is represented.
- (ii) macroscopic: disregarding the internal geometry and obtaining the mean behaviour.

The microscopic scale is not practical for typical coastal engineering problems for many reasons. First of all, it is hard to assess and survey the exact geometry within a porous medium. Next to that it is computationally very expensive to capture all the scale grades, from armour units to sand, in a mesh. And finally, the interest lays in the overall influence of the porous media, not so much in the precise pore velocity in a specific location.

The macroscopic scale averages and as it filters out small-scale variations associated with the irregular media. The modelling of waves and porous media interaction is based on the coupling of two flow models: one that describes the flow in the outer region acting on the structure and one that describes the spatially averaged flow through the porous material. The quality of the modelling will be limited by the simplifications formulated for the flow in the outer fluid region; by the validity, hypotheses, and parameterisation of the porous flow model, which usually relies on some constants depending on the flow (Inigo J Losada et al. 2016).

The Navier-Stokes (NS) equations for porous flow is the starting point to derive a set of equations able to model flow in varying detail and precision in porous media. The following solutions have been derived:

- Solutions based on linear wave theories

- Solutions for simple geometries based on eigenfunction expansions
- Solutions based on the mild-slope equation
- Advanced depth integrated models
  - Nonlinear shallow water and Boussinesq-type models
- Models based on NS equations
  - Eulerian NS models
  - Lagrangian NS models

## 2.4.2 Strengths and limitations

Before the exponential increase of computational power of the last decade, practical numerical modelling tools used to be limited to Boussinesq-type (like Sørensen, Schäffer, and Madsen 1998) or statistical modelling of the wave field (Niels G. Jacobsen, Fuhrman, and Fredsøe 2012). They have their limitations, for example: they are unable to model overturning waves and as a consequence cannot model pressures and force magnitudes of the water acting on the structure. That is a consequence of the fact that they are depth-integrated and the fact that they rely on potential flow theory. Another drawback for Boussinesq models or other wave theories, is that wave breaking process must be triggered artificially (Inigo J Losada et al. 2016). These drawbacks apply even more so on models using the solutions based on linear wave theories.

Much freedom is acquired by using the free surface modelling based on the Reynolds-Averaged Navier-Stokes equations (RANS). The use of RANS equations to model coastal engineering processes is growing in importance. One of their greatest features is the capability to obtain three dimensional pressure and velocity profiles, which allow for a more realistic simulation of wave conditions along the whole spectrum of relative water depth. The Eulerian approach makes it easier to track magnitudes in any point of the mesh as it is continuous. The lagragian approach show great early results, but is still in a very early stage of validion for real applications (Higuera, Lara, and Inigo J. Losada 2013). The biggest drawback of the free surface models based on the RANS equations is that these are computationally expensive.

Today’s commercial CFD packages increase in cost with the number of applied processors, whereas the expenses for hardware are reasonable (Niels G. Jacobsen, Fuhrman, and Fredsøe 2012). The additional vertical dimension comes at a computational cost and large computational demands typically require software which can run parallel. In recent years, the freely available CFD library OpenFoam® has gained popularity, and active communities have appeared. At the moment, it is increasingly used by practising engineers, as well as researchers.

A key element for coastal engineering studies is the ability to generate and absorb surface water waves in a flexible manner. The modelling of propagating water waves in OpenFoam has previously been studied, however, they suffered from the lack of outlet relaxation zones, and the relaxation technique suffers from a requirement of highly refined computational meshes around the water surface. Both of these limitations are addressed and solved in the present work. This has been solved by Niels G. Jacobsen, Fuhrman, and Fredsøe 2012. They have developed a tool called waves2Foam which makes use of the relaxation zone technique and coupled with the standard volume of fluid (VOF) scheme in OpenFoam, is demonstrated to accurately model propagating and breaking waves. It is made freely available for the community.

The biggest drawback of the currently available versions of OpenFOAM® and the waves2Foam toolbox is that it is not capable of simulating the movement of the porous layer itself. For example, the dynamic development of the cross shore profile during a simulation cannot be modelled.

## 2.5 Conclusions

The drawn conclusions are:

- Formulae trying to predict overtopping discharges have fitted empirical expressions to overtopping data of laboratory experiments. Few experiments have measured overtopping on cobble revetments, and those that have are not applicable to the Maasvlakte II case as Iribarren numbers, cobble diameters, cobble layer thicknesses and core characteristics are significantly different.
- Studies haven't incorporated the specific influence of varying porosity or layer thickness of cobble layers on the overtopping. Only one study has looked at the effect of absorption of up rushing water on the overtopping water on a hollow concrete blocks.
- Many studies have been conducted on the relation between cross shore morphodynamics of cobble layers and sand washing-in to its pores.
- OpenFOAM® with the waves2Foam toolbox is a free surface modelling tool based on the Reynolds-Averaged Navier-Stokes equations and can simulate porous media flow and wave conditions along the whole spectrum of relative water depth.
- OpenFOAM® cannot model the cross shore morphodynamics of the cobble layer when exposed to waves during a simulation, as cobble transport is not accounted for.
- The contractor has completed many physical model tests at certified institutions looking into the cross shore morphology related to sand content in the cobble layer. The maximum sand content was 50%, but during site inspections much higher contents have been observed.

The conclusions show a significant knowledge gap. The general characteristics of cobble revetments as a whole have been a region of active research. It is, however, unknown what the exact quantitative influence of a decrease of porosity and a reduced effective cobble layer thickness as a result of sand washing is on overtopping. The increase of computational power and decrease of costs make the use of highly detailed depth resolving CFD models such as OpenFOAM an attractive endeavour. The advantage of physical model over numerical tests is that it's closer to reality, as cobbles can migrate during the simulation. The drawbacks are that modelling at the scale required ( $N_L \leq 5.5$ ) to reasonably model the interaction between sand and cobbles is costly, time consuming, susceptible to breakdowns and for this research simply unfeasible.

The experimental data produced by the numerical model can be used to (i) shed light on the case study of the Maasvlakte II revetment, and (ii) to formulate  $\gamma_f$  as a function of relative pore volume per revetment area. This empowers researches, as well as practising engineers to predict overtopping discharges on cobble revetments with varying porosity and cobble layer thickness with impermeable cores with more precision.

Authors	Formulae	Breaking type
Wassing (1957)	$R_{u2\%} = 8H_{1/3} \tan \alpha$	breaking
Ahrens (1981)	$\frac{R_{U2\%}}{H_{m0}} = 1.6\xi_{0p}$	breaking
	$\frac{R_x}{H_{m0}} = C_1 + C_2(H_{m0}/gT_p^2) + C_3(H_{m0}/gT_p^2)^2$	non-breaking
Mase (1989)	$\frac{R_{U2\%}}{H_{m0}} = 1.86\xi_{0p}^2$	breaking
Van der Meer (1992)	$\frac{R_{U2\%}}{H_s} = 1.5\gamma\xi_p$ , with maximum of 3.0	breaking and non-breaking
Burchart and Hughes (2002): Coastal Engineering manual	$\frac{R_{U2\%}}{H_{m0}} = 1.6\xi_{0p}$	breaking
	$\frac{R_{U2\%}}{H_{m0}} = 4.5 - 0.2\xi_{0p}$	non-breaking
Hughes (2004)	$\frac{R_{U2\%}}{h} = 4.4(\tan \alpha)^{0.7} \left(\frac{M_f}{\rho gh^2}\right)^{1/2}$	breaking
	any value of $H_{m0}/L_p$ and $1/30 \leq \tan \alpha \leq 1/5$	
	$\frac{R_{U2\%}}{h} = 4.4(\tan \alpha)^{0.7} \left(\frac{M_f}{\rho gh^2}\right)^{1/2}$	breaking
	$H_{m0}/L_p > 0.0225$ and $1/5 \leq \tan \alpha \leq 2/3$	
	$\frac{R_{U2\%}}{h} = 1.75(1 - e^{(-1.3 \cot \alpha)}) \left(\frac{M_f}{\rho gh^2}\right)^{1/2}$	non-breaking
	$H_{m0}/L_p < 0.0225$ and $1/4 \leq \tan \alpha \leq 1/1$	
Eurotop (2007)	$\frac{R_{U2\%}}{H_{m0}} = 1.6\xi_{m-1.0}$	breaking
	$\frac{R_{U2\%}}{H_{m0}} = 4.0 - \frac{1.5}{\sqrt{\xi_{m-1.0}}}$	non-breaking

Table 2.1: A summary of the most relevant formulae predicting run-up resulting from irregular waves on smooth impermeable slopes (Arana, 2017)

Authors	Formulae	Structure type
Owen (1980)	$\frac{Q}{T_m \cdot g \cdot H_{m0}^3} \cdot \sqrt{\frac{s_{0m}}{2\pi}} = A \cdot \exp\left(-B \frac{R_c}{H_{m0}} \sqrt{\frac{s_{0m}}{2\pi}} \frac{1}{\gamma_r}\right)$ <p><math>0.50 \leq \gamma_r \leq 0.55</math> for two layers of rock armour</p>	straight slopes
Besley's (1999) correction of Owen (1980)	$C_r = \min\left[3.06 \cdot \exp\left(-1.5 \frac{G_C}{H_{m0}}\right); 1\right]$ <p>multiply reduction factor, <math>C_r</math> with <math>Q</math></p>	berm slopes
Van der Meer & Janssen (1994)	$\frac{Q}{g \cdot H_{m0}^3} \cdot \sqrt{\frac{s_{0p}}{\tan \alpha}} = 0.06 \cdot \exp\left(-5.2 \frac{R_c}{H_{m0}} \frac{\sqrt{s_{0p}}}{\tan \alpha} \frac{1}{\gamma}\right)$ <p><math>\gamma = \gamma_r \cdot \gamma_b \cdot \gamma_h \cdot \gamma_\beta</math></p>	breaking waves
Hebsgaard et al. (1998)	$\frac{Q}{g \cdot H_{m0}^3} \cdot \frac{1}{\ln s_{0p}} = k_1 \cdot \exp\left(k_2 \cdot \frac{\cot^{0.3} \alpha \cdot (2 \cdot R_c + 0.35 \cdot G_c)}{H_{m0} \cdot \cos \beta}\right) \cdot \frac{1}{\gamma_r}$ <p><math>k_1 = -0.3</math> and <math>k_2 = -1.6</math></p>	rubble mound
Eurotop (2018)	$\frac{Q}{g \cdot H_{m0}^3} = \frac{0.023}{\sqrt{\tan \alpha}} \cdot \gamma_b \cdot \xi_{m-1.0} \cdot \exp\left[-\left(2.7 \frac{R_c}{\xi_{m-1.0} \cdot H_{m0} \cdot \gamma}\right)^{1.3}\right]$ <p>with a max of: <math>\frac{Q}{g \cdot H_{m0}^3} = 0.09 \cdot \exp\left[-\left(1.5 \frac{R_c}{H_{m0} \cdot \gamma_f \cdot \gamma_\beta \cdot \gamma^*}\right)^{1.3}\right]</math></p> <p><math>\gamma = \gamma_b \cdot \gamma_f \cdot \gamma_\beta \cdot \gamma_v</math>; formulae state the mean value approach</p>	various materials and configurations

Table 2.2: An overview of the most relevant formulae predicting overtopping resulting from irregular waves

## Chapter 3

# Laboratory Experiments

The aim of this chapter is to analyse the physical experimental data, so a validation of the numerical model in chapter 4 is facilitated. In the first section the context of the experiments is stated, then in the second section the experimental procedures are explained. After that, the criteria to enable successful numerical validation are described in section 3.3 and finally, in section 3.4, key characteristics of the data and the laboratory effects are stated.

### 3.1 Context

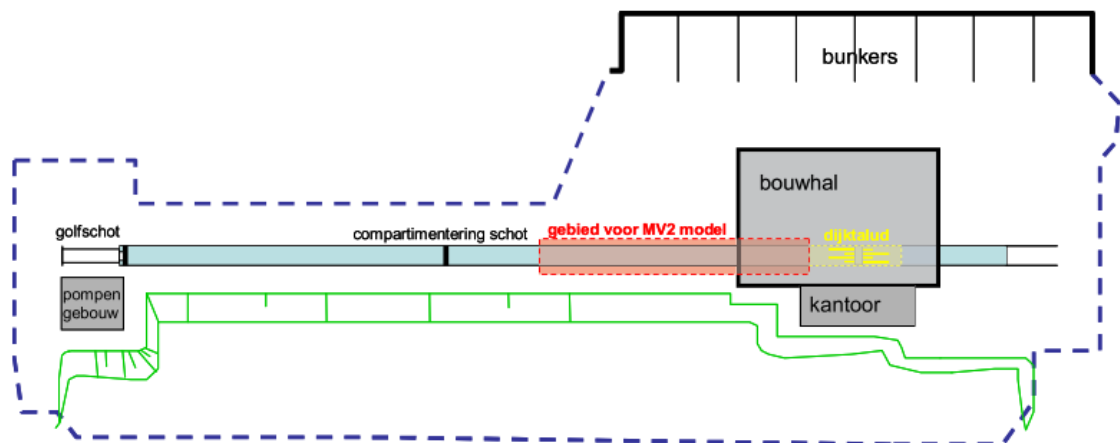


Figure 3.1: Plan of Delta flume at Marknesse.

Because of the required minimum scale, determined by the suspension scaling of the sand with an average prototype  $d_{n,50}$  of  $370 \mu m$ , PUMA selected Deltares (previously called Delft Hydraulics) to carry out the physical 2D model tests in the large wave flume Deltagoot at a geometric scale  $N_L$  1 in 5.5. This wave flume at Marknesse, the Netherlands, was 240 meter long, 5 meter wide and 7 meter deep, and was able to generate irregular waves with a maximum wave height up to 2.5 meter.

## 3.2 Experimental procedures

The experiments consisted of measuring the deformed cross-shore profile, as well as the wave overtopping volume as a result of inbound irregular waves. Here, the storm condition curve has been schematised into five constant wave conditions steps (each of three hours), lasting from 10.5 hours before to 4.5 hours after the storm peak. Figure 3.2 shows the wave spectrum of the the tested storm conditions. The verification criteria of the experiments at that time were that during the tests:

- the sand underneath the cobble layer does not disappear;
- the wave overtopping does not exceed a specific discharge limit.
- sand underneath the cobble layer does not wash out.

In total five test series have been conducted, comprising of varying cross sections and varying amounts of sand washed-in to the cobble profile. Each test series have been labelled by the following code  $S_xT_y$ ; with  $x$  being the test series number and  $y$  being the wave condition as specified in figure 3.2.

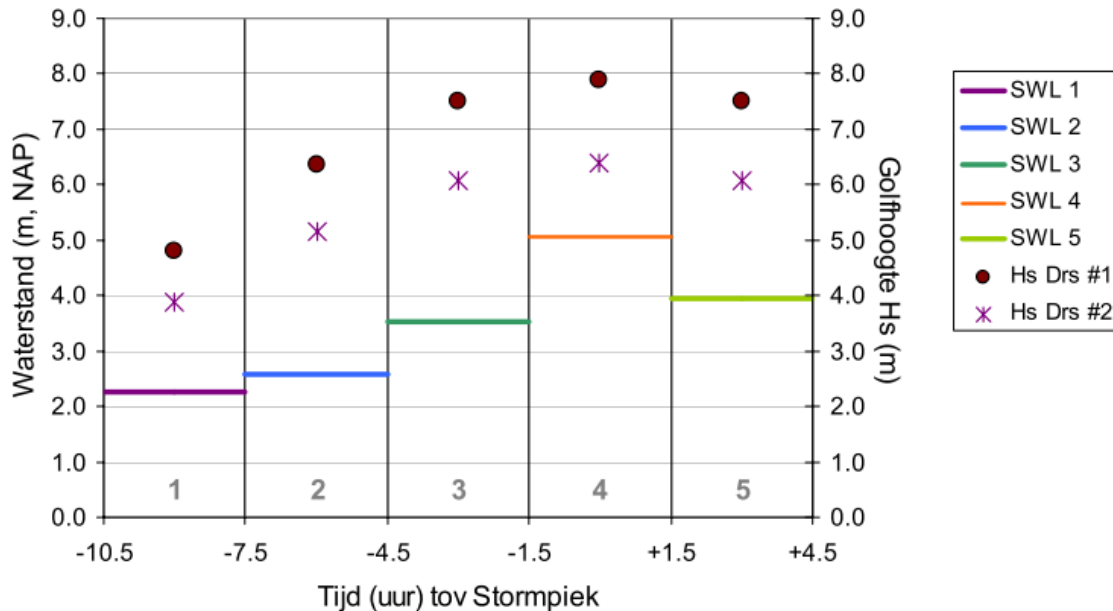


Figure 3.2: Overview of the physical model test wave conditions on prototype scale.

## 3.3 Criteria for the experimental data for numerical validation

The purpose of the experiments have been stated clearly in section 3.2. At that time there were no intentions on generating and carefully logging data high resolution for the use of the validation of CFD models. Ideally one would have the velocity signal of the wave paddle of each of the tests, as well as the corresponding run-up and overtopping measurements over time to compare the physical data next to the experimental data in a time domain. That allows for shorter simulation times which is computationally more

efficient. However, these were not available.

The data that is available of the five test series are the wave conditions, profile deformations and overtopping after each wave condition test of 3 hours (prototype scale). The criteria to identify the most useful test step of the series from which the data can be used to validate the results of the numerical model were the following:

- Overtopping must occur, e.g. if no overtopping events take place there is not sufficient data available to validate the numerical results of the OpenFOAM model other than the fact that there is not any overtopping.
- An experiment where a cobble profile in which sand is washed-in. OpenFOAM should adequately model flows in porous media partly filled with sand.
- An experiment where a cobble profile in which no sand is washed in. OpenFOAM should adequately model flows in porous media.

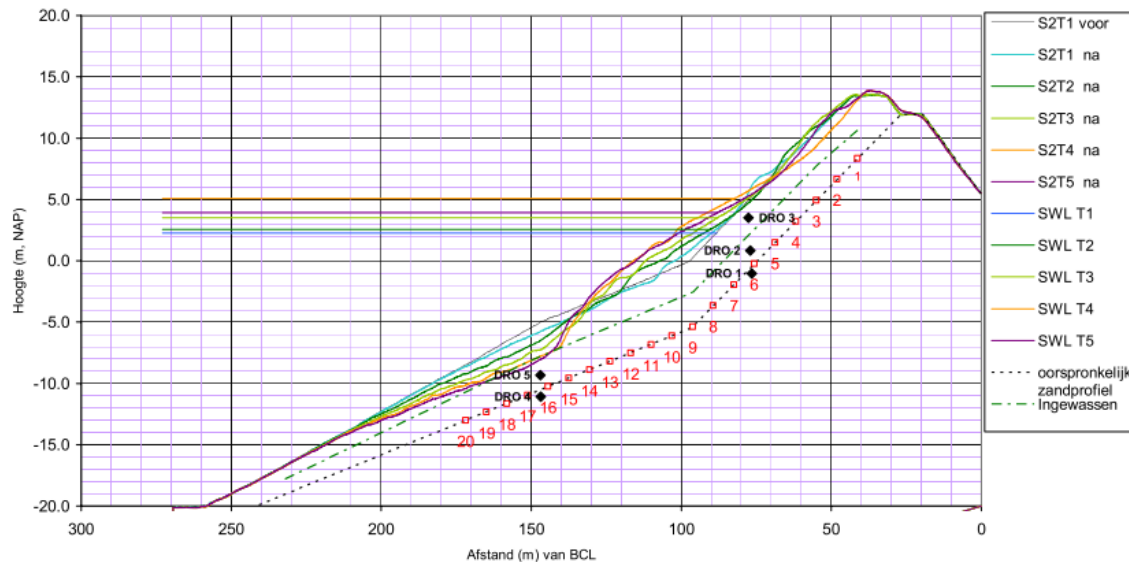


Figure 3.3: Overview of the average cross shore profiles after each of the wave conditions during S2 experiments (prototype dimensions).

### 3.4 Experimental data

See table 3.1 for an overview of all the relevant parameters other than the cross shore profile of the revetment. In the test series the irregular wave conditions followed a JONSWAP spectrum with peak enhancement factor  $\gamma = 2.2$ . Test S2T4 has the largest specific overtopping discharge, as well as partly sanded in cobble profile, therefore the most suitable experiment to reproduce numerically after which results can be compared. Deltares has provided surface elevation time series of three wave gauges along the flume. The spectral energy density curve has been calculated.

Test S1T4 has no sand washed-in to the cobble revetment and still some overtopping is measured during the experiments. Deltares has not provided surface elevation data, however wave data can be considered fairly similar.

Target conditions			
SWL	[m, NAP]	0.92	
Bottom level	[m, NAP]	- 3.64	
$H_{m0}$	[m]	1.42	
$T_{m-1,0}$	[s]	4.95	
$T_p$	[s]	5.76	
Duration	[min]	76.8	
Measurements		<b>S1T4</b>	<b>S2T4</b>
$H_{m0}$	[m]	1.43	1.42
$T_{m-1,0}$	[s]	5.16	5.16
$T_p$	[s]	5.76	5.76
$q$	[l/m/s]	0.18	0.50
$n_p$	[-]	0.30	0.32
$D_{n,50}$	[m]	0.0146	0.0152

Table 3.1: A summation of the target conditions and measured results from test S1T4 and S2T4 on model scale. The specific discharge  $q$  is calculated based on total overtopping volume divided by the time and the width of 1m the asymmetrical west part of the revetment where most of all the overtopping occurred.

### 3.4.1 Profile asymmetry

During both the S1 and S2 series the incoming waves reshaped the cobble revetment significantly. However, already at the very start of the tests wave run-up was not symmetrical. The cause is hard to pinpoint exactly; it could have been small deformations during construction. The run-up at the west side of the revetment was somewhat higher than the middle and east side. The increased velocities and discharge translated to more erosion at the west part of the top and as a result the bulk of the overtopping occurred on the west side of the revetment, see figure 3.4. The specific overtopping discharge,  $q$ , is calculated based on total overtopping volume divided by the time and the width of 1m of this asymmetrical west part of the revetment.



Figure 3.4: Asymmetrical profile development during the S1 test series.

## Chapter 4

# Numerical experiments

### 4.1 OpenFOAM, Waves2Foam and OceanWave3D

OpenFOAM (Open source Field Operation And Manipulation) is a C++ toolbox for the development of customized numerical solvers, and pre-/post-processing utilities for the solution of continuum mechanics problems, including computational fluid dynamics (CFD). The code is released as free and open-source software under the GNU General Public License. OpenFOAM has been released by OpenCFD since 2004, the name OpenFOAM was registered as a trademark by OpenCFD Ltd in 2007 and has been non-exclusively licensed to the OpenFOAM Foundation Ltd since 2011.

The library waves2Foam is a toolbox for OpenFOAM used to generate and absorb free surface water waves Niels G. Jacobsen, Fuhrman, and Fredsøe 2012. Currently the method applies the relaxation zone technique (active sponge layers) and a large range of wave theories are supported and the relaxation zones can take arbitrary shapes. It is originally developed at the Technical University of Denmark by Niels Gjøel Jacobsen under supervision of Prof. Jørgen Fredsøe. In 2014 the porosity module was developed to model the interaction between free-surface waves and a permeable medium in collaboration between Bjarne Jensen and Niels Gjøel Jacobsen, both then at the university of Denmark. Now further developments take place at Deltares, Niels G. Jacobsen's current employer.

Fully nonlinear waves can be computed with the wave transformation model OceanWave3D Engsig-Karup, H. B. Bingham, and Lindberg 2009. The coupling between OceanWave3D and OpenFoam is already implemented in waves2Foam following the work by Paulsen, Bredmose, and Harry B. Bingham 2014. This approach allows for an efficient use of computational resources. In view of the very large number of waves to be simulated (we recall that the irregular wave signal consists of hundreds of waves), it is prohibitively expensive to compute the waves with the OpenFoam model all the way from the paddle to the structure.

### 4.2 Numerical model

The numerical framework is OpenFOAM version foam-extend-3.1 and the framework provides the means of solving free surface flows with the volume of fluid method (VOF). Based on the experiments performed in the Delta Flume described in chapter 3, the model needs to meet the following requirements: (i) solution to the Navier-Stokes equations in- and outside of a permeable layer, (ii) tracking of the free surface in- and outside of a permeable layer and (iii) generation and absorption of free surface waves.

### 4.2.1 Navier-Stokes equations

Jensen, Niels Gjøøl Jacobsen, and Christensen 2014 presented a form of the Navier-Stokes equations that accounts for the presence of permeable coastal structures. It has been successful in describing the interactions between waves and breakwaters (Niels G. Jacobsen, M. R. v. Gent, and Wolters 2015) and also in validating wave-induced pressures in an open filter. The Navier-Stokes equation took the following form:

$$(1 + C_m) \frac{\delta}{\delta t} \frac{\rho \mathbf{u}}{n_p} + \frac{1}{n_p} \nabla \cdot \frac{\rho}{n_p} \mathbf{u} \mathbf{u}^T = -\nabla p^* + \mathbf{g} \cdot \mathbf{x} \nabla \rho + \frac{1}{n_p} \nabla \cdot \Gamma_u \nabla \mathbf{u} - \mathbf{F}_p \quad (4.1)$$

Where  $\delta$  is the added mass coefficient,  $t$  is time,  $\rho$  is the density of the fluid,  $\mathbf{u}$  is the filter velocity vector,  $n_p$  is the porosity of the permeable structure,  $p^*$  is an excess pressure,  $\mathbf{g}$  is the vector due to the acceleration of gravity,  $\mathbf{x}$  is the Cartesian coordinate vector,  $\Gamma_u$  is the diffusivity of the velocity field and  $F_p$  is the resistance force due to the permeable structure. The system of equations is closed with the incompressible form of the continuity equation:

$$\nabla \cdot \mathbf{u} = 0 \quad (4.2)$$

The Darcy-Forchheimer flow resistance formulation describes the flow resistance term in equation 4.1:

$$\mathbf{F}_p = \rho a \mathbf{u} + \rho b \|\mathbf{u}\|_2 \mathbf{u} \quad (4.3)$$

The closure coefficients  $a$  and  $b$  are evaluated based on the parameterisation by M. v. Gent 1995:

$$a = \alpha \frac{(1 - n_p)^2}{n_p^3} \frac{v}{D_{n,50}^2} \quad \text{and} \quad b = \beta \left( 1 + \frac{7.5}{KC} \right) \frac{1 - n}{n^3} \frac{1}{D_{n,50}^2} \quad (4.4)$$

Where  $v$  is the kinematic molecular viscosity,  $D_{n,50}$  is the nominal diameter of the permeable layer,  $KC$  is the Keulegan-Carpenter number and  $\alpha = 1000$  and  $\beta = 1.1$  are the closure coefficients.

### 4.2.2 Turbulence and resistance parameters

No separate turbulence model is used for the simulations. The Darcy-Forchheimer equation was introduced to the Navier-Stokes equations as a closure model for handling the porous media resistance force which cannot be resolved directly in the model. If the resistance coefficients,  $\alpha$  and  $\beta$ , are found from measurements they already include the effect of turbulence (Jensen, Niels Gjøøl Jacobsen, and Christensen 2014), see section 6.3 for a discussion.

It should be noted that uncertainties are related to the magnitude of  $\beta$  and the  $KC$  number. The main reason for this is the lack of spatial and temporal variation in  $KC$ . The  $KC$  number is evaluated based on linear wave theory at the toe of the structure, where the maximum orbital velocity is an approximation to the pore velocity in the top part of the filter. These uncertainties will affect the results quantitatively. However, as Niels G. Jacobsen, M. R. v. Gent, and Wolters 2015 notes, no data was available for the calibration of the velocities inside of the rock layer, while a validation of the wave-induced pressures inside an open filter is already performed based on the chosen approach for  $\beta$  and  $KC$ .

Some debate exists concerning the standard values of  $\alpha$  and  $\beta$ . For an extended discussion on this topic please look to the work of Inigo J Losada et al. 2016, Higuera, Lara, and Inigo J. Losada 2013.

### 4.2.3 Tracking of the free surface

An advection algorithm named MULES tracks the free surface. It's the standard method available in OpenFOAM. The equation is:

$$\frac{\delta F}{\delta t} + \frac{1}{n_p} \left[ \nabla \cdot \mathbf{u}F + \nabla \cdot \mathbf{u}_r(1 - F)F \right] = 0 \quad (4.5)$$

$F$  is the indicator function of the Volume of Fluid (VOF) field and  $\mathbf{u}_r$  is a relative velocity introduced to keep a sharp interface. See Rusche and Berberovic et al. for details. The factor  $1/n_p$  has been introduced by Jensen, Niels Gjøøl Jacobsen, and Christensen 2014 to ensure conservation of mass when fluid passes through a permeable structure. The indicator function is applied to evaluate the spatial variation of the density and the viscosity:

$$\rho = F\rho_1 + (1 - F)\rho_0 \quad \text{and} \quad \Gamma_u = F\Gamma_{u,1} + (1 - F)\Gamma_{u,0} \quad (4.6)$$

The sub-indices refer to the fluid properties for  $F = 0$  and  $F = 1$ . In this work we choose a similar definition as presented by Jensen, Niels Gjøøl Jacobsen, and Christensen 2014 and Niels G. Jacobsen, M. R. v. Gent, and Fredsøe 2017,  $F = 1$  means that the computational cell is filled with water and  $F = 0$  means that the cell is filled with air. A cell with a value of  $F$  between 0 and 1 will be located at or very close to the free surface. Furthermore, a free surface cell can be identified being a cell with a non-zero  $F$  and having at least one neighbouring cell where  $F = 0$ .

### 4.2.4 Generation of free surface waves

The waves2Foam toolbox for OpenFOAM (Niels G. Jacobsen, Fuhrman, and Fredsøe 2012) generate and absorb the free surface waves. It is based on a relaxation technique, where the weighting is responsible for compensation of the inward Stokes drift such that no accumulation of water inside the domain occurs. Unless otherwise specified, the irregular wave field is generated based on a linear superposition of the individual frequencies in the wave spectrum. A total of 100 wave components together make up the JONSWAP spectrum with a peak enhancement factor of  $\gamma = 2.2$ . The frequencies are non-equidistantly distributed with a higher frequency resolution around the peak of the spectrum than at the tails. This enables a better time domain representation of the exceedance statistics of wave height and wave periods for a small number of frequencies.

### 4.2.5 Measuring overtopping

From the waves2FOAM manual by Niels Gjøøl Jacobsen 2017: "Overtopping is the amount of water that is overtopping the structure. This functionality is used in run-time, as the process of overtopping is very rapid. Consequently, the overtopping is evaluated at every time step. During the simulation the following types of face fluxes are available:

- $\phi$  in [ $m^3/s$ ] is the flux of fluid across a face;
- $\phi_\rho$  in [ $kg/s$ ] is the flux of fluid across a face multiplied by the density of the fluid;
- $\phi_F$  in [ $m^3/s$ ] is the flux of fluid across a face multiplied with the indicator function.

While a combination of  $\phi$  and  $\phi_F$  would be perfect to evaluate the flux of water across a face this is not possible, as  $\phi_F$  is not available throughout the entire time step; consequently

it is not available when the function objects are evaluated. Therefore, the flux of water is estimated with the use of  $\phi$  and  $\phi_\rho$  instead. In the solution to the advection of the indicator function the following relationship is used:

$$\phi_\rho = (\rho_{F=1} - \rho_{F=0})\phi_F + \rho_{F=0}\phi \quad (4.7)$$

Now,  $\phi_F$  can be estimated as follows

$$\phi_F = \frac{\phi_\rho - \rho_{F=0}\phi}{\rho_{F=1} - \rho_{F=0}} \quad (4.8)$$

Knowing the flux of water (assuming that the fluid is water, when  $F=1$ ), it is now possible to evaluate the overtopping over a set of faces,  $\Upsilon$ :

$$\mathbf{q} = \sum_{f \in \Upsilon} \phi_{F,f} \frac{S_f}{\|S_f\|_2} \quad (4.9)$$

where  $\mathbf{q}$  is the volume flux in [ $m^3/s$ ] and  $S_f$  is the non-unit normal vector to the face. Here,  $\phi_F$  is positive in the direction of the normal vector and negative in the opposite direction, so the combination gives the directional overtopping over a set faces.

## 4.3 Setup for the simulations

### 4.3.1 Domain

The mesh or grid is an integral part of the numerical solution and must satisfy certain criteria to ensure a valid approximation of the solution. During any run, OpenFOAM checks that the mesh satisfies a fairly stringent set of validity constraints and will cease running if the constraints are not satisfied.

The domain starts at  $x = 103\text{m}$  and ends at  $x = 174$ . The bottom of the flume and domain is at  $y = -3.67\text{m}$  and the top of the domain is at  $y = 4.67\text{m}$  and the mesh is created by the *BlockMesh* application.

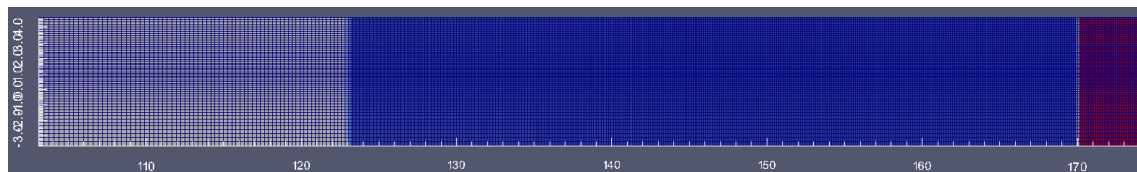


Figure 4.1: Overview of the numerical grid in Paraview. Note the non-equidistant gridsizes, the relaxation zone inlet in white and the relaxation zone outlet in red.

### 4.3.2 Revetment

The revetment consists of cobbles deposited on a sand core. The sand on which the cobble layer lays can be considered impermeable with respect to the wave period. This is beneficial, because now the cells within the sand layer can be cutoff and thereby reducing the amount of grid cells. See fig 4.6 for the grid. The height of the sand layer can be altered for each simulation, thereby implicitly changing the thickness of the cobble layer. For each simulation a different grid can be constructed. This is facilitated by the *snappyHexMesh* application which can cut away, refine and modify cells of the grid according to predefined coordinates or structures.

### 4.3.3 Time step

A indicative time step is programmed for each simulation in the order of  $\Delta t = 0.001s$ . However, the time step can be increased by OpenFOAM itself until it reaches its maximum at  $\Delta t < 0.35 \cdot CFL$ . Since the adaptive time-step method is Courant number based, the time-step can go to extremely high values as the simulations starts as there are no high velocities present in the simulation. Mathematically it could be correct, however, it contradicts the physics of the wave propagation phenomena. This issue can be resolved by using a  $\Delta t_{max}$  parameter or using a fixed time-step for a while. Similar conclusion were drawn by Berberović et al. 2009.

### 4.3.4 Boundary conditions

Relaxation zones at the inlet and outlet boundary. The upper atmosphere boundary condition imposes an atmospheric pressure corrected for the square of the velocity. The air and water can freely exit, while only air can flow in. The bottom boundary is a closed boundary.

	input	symbol	unit	value
	porosity	$n_p$	[-]	0.32
	Karpegan-Ceuler number	$KC$	[-]	10000
cobbles	median cobble diameter	$D_{n,50}$	[m]	0.015
	alpha	$\alpha$	[-]	1000
	beta	$\beta$	[-]	1.1
	spectrum type			Jonswap
	depth	$h$	[m]	4.56
waves	spectral shape factor	$\gamma$	[-]	2.2
	spectral wave height	$H_{m0}$	[m]	1.42
	spectral peak period	$T_p$	[s]	5.76
	random phase seed		[-]	30
	timestep	$\Delta t$	[s]	$0.35 \cdot CFL$
system	turbulence model			laminar
	simulation duration	$t_{simulation}$	[s]	1600
	solver		[-]	Interfoam

Table 4.1: Overview of the inputs used for the mesh study and validation of the simulations.

## 4.4 Mesh study

The right mesh is indispensable for correct numerical results. In Appendix B the design is explained, then the quality of the meshes is assessed based on (i) rate of convergence, (ii) solution precision and (iii) CPU time required. This is done for two zones of interest: (a) the start of the domain just next the relaxation zone until the toe of the revetment for

wave propagation processes, and (b) the top half of the revetment where wave breaking as well as wave overtopping occurs.

This section is positioned here before the section in which the validation is set out, though, in reality it is an iterative process. For an overview of the input parameters is referred to section 4.5.

#### 4.4.1 Conclusion

GB01, as can be seen in table B.2 and B.3, is a suitable mesh for cases where consistent overtopping is expected and is the mesh which is used for all the simulations in this work, except for cases VS13 and VS14. A higher resolution, such as simulation GB03, comes at almost three times the computational cost, but approximates the solution just slightly better. This mesh is therefore used in the VS13 and VS14 simulations aiming to reproduce the overtopping discharge as measured in the physical experiment, see section 4.5. In simulations where overtopping events are expected to be scarce and volumes are relatively low, it is better capable of capturing the small quantities of water topping over as the estimation of the fluid flux across a face multiplied with the indicator function is more precise.

case ID	$N_x$	$N_y$	# cells	$\frac{H_{m0}}{\Delta y_{swl}}$	$\frac{L}{\Delta x_{toe}}$	$\frac{L}{\Delta x_{crest}}$	$\frac{t_{clock}}{t_{simulation}}$ [min/s]
GB01	300	42	12420	9	81	203	1.30
GB03	400	55	21693	11	108	271	2.63

Table 4.2: Overview of the two meshes used for the numerical simulations and their dimensionless characteristics.

## 4.5 Validation with respect to the overtopping

The correct working of the numerical model is proven by validating the results with the data from test S1T4 and S2T4 described in chapter 3. Several subjects concerning the validation will be explained in the next sections. First the wave conditions are touched upon, after which the layouts of the numerical revetments are clarified. Then the characteristics of the porous layers in OpenFOAM are explained and finally a comparison of the numerical specific overtopping discharges and the experimental overtopping is made.

### 4.5.1 Wave conditions

As it has not been possible to obtain the original velocity signal of the wave paddle, the inbound irregular waves are not an identical realisation of the surface elevation, but a different realisation of the same energy density spectrum. The inbound waves are statistically very similar, i.e. the energy density spectrum of the numerical surface elevation measured by numerical wave gauges (see figure 4.2 for an overview) is almost a good reproduction of the data in terms of statistical parameters of test S2T4 provided by Deltares (see figure 4.3b). The downside of a comparison in this framework is that long simulations (1600s or

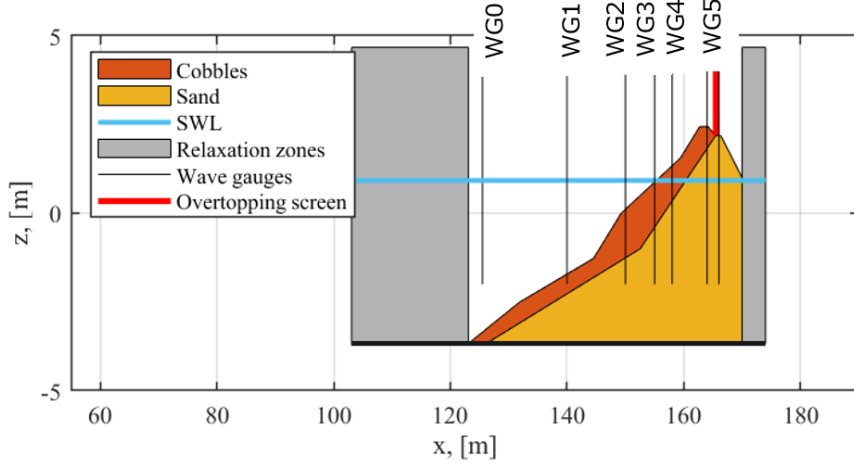
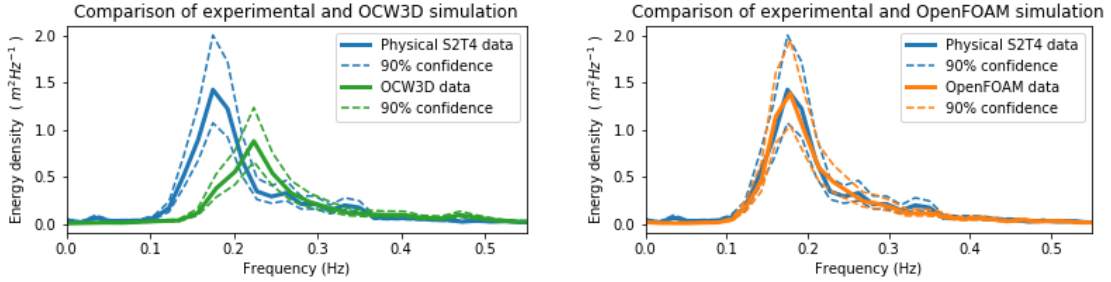


Figure 4.2: Cross shore profile of the numerical setup. The sand is hydraulically impermeable, the median cobble diameter  $D_{n,50} = 0.015m$ . The numerical wave gauges are shown in this plot.

25 min) are needed so to obtain enough waves to acquire a decent frequency resolution  $\delta f$ , as well as an acceptable reliability interval. This is a rather computationally expensive endeavour.



(a) Potential wave theory with domain length  $x = 230$  m and  $h = 4.56$  m and with the amount of grid points evenly distributed  $N_x = 1200$  and  $N_y = 30$ . The numerical wave gauge is positioned at  $x = 77$  m, a simulation time of  $t = 1640$  s and a varying numerical time step such that  $CFL < 0.85$

(b) Depth resolving model with domain length  $x = 104 - 174$  m and  $h = 4.56$  m and with the amount of grid points unevenly distributed  $N_x = 300$  and  $N_y = 42$ . The numerical wave gauge is positioned at  $x = 123.51$  m, a simulation time of  $t = 1640$  s and a varying numerical time step such that  $CFL < 0.35$

Figure 4.3: A comparison of the energy density spectra of the numerical and experimental tests.

The energy density spectrum of OCW3D does not correlate with the energy density spectrum of the experimental data when irregular waves according to the identical distribution are generated (see figure 4.3a). Also, statistical wave parameters such as significant wave height,  $H_s$  are do not compare with each other. At this time it is not known what the reason is for this mismatch. Hereafter the OCW3D module, responsible for modelling the transmission between the numerical wave creation zone and the revetment, is omitted from the model setup. The waves are generated in the relaxation zone between  $x=104$

and  $x=124$ , see fig. 4.2. Deltares has been informed of this error and hasn't been solved yet at the time of writing.

## 4.5.2 Numerical representation of the revetment

### Cross shore profile

OpenFOAM cannot model the movement of the cobbles and as a result the morphodynamics of the cobble layer during the experiments is not captured. Therefore, for each of the validation experiments two cross shore profiles of the cobble layer were used in the simulations: (a) the profile measured before the experiment, and (b) the profile measured after the experiment. The specific overtopping discharges,  $q$ , measured during the simulations were averaged with the following weighting:  $1/3 \cdot q_a$  and  $2/3 \cdot q_b$  and then compared with the Deltares data. The weighting was applied as the dynamic behaviour of the cross shore profile at the start of the experiment is larger than the at the end (M. v. Gent 2009), see section 5.1 for an discussion.

### Profile asymmetry

The run-up and overtopping at the west side of the revetment of the wave flume during both the S1 and S2 series was higher than that on the middle and east side. The height and cross shore shape of the profiles in OpenFOAM has been based on the west part of the revetment as it is the location where most overtopping occurs and it is this width of 1m that the specific discharge  $q$  is calculated which is specified in the data provided by Deltares.

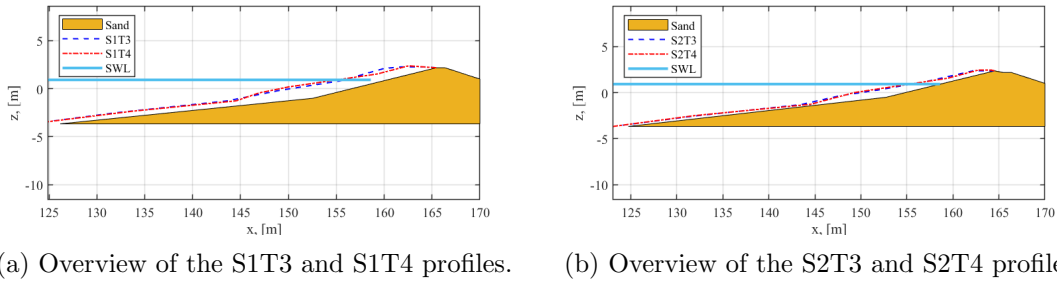
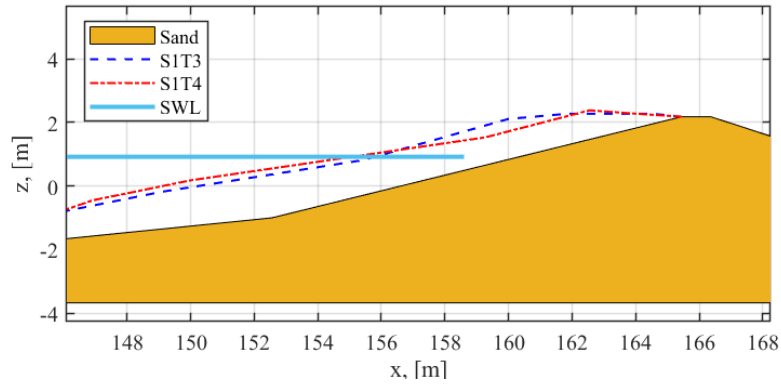


Figure 4.4: An overview of the cross shore profiles as measured by Deltares. Note the decrease in thickness of the effective cobble layer for the S2 profiles

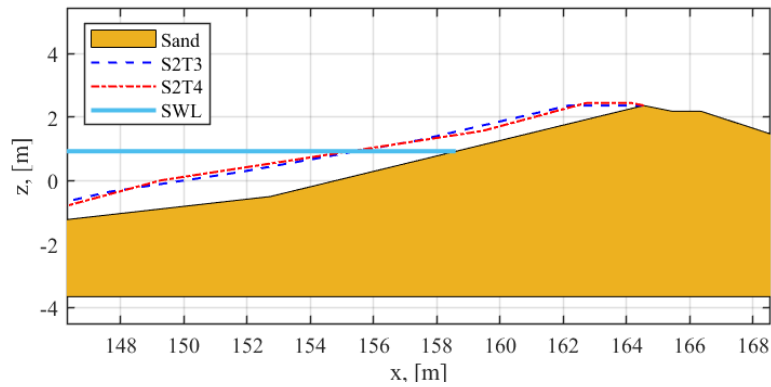
### Numerical shape

The cross-shore design of the revetments in the numerical simulations are a reproduction of the layout of the revetment measured in the physical experiments. The washed-in sand level, the sand level, thickness and the shape of the cobble layer after the physical experiments have been provided and measured by Deltares.

The computational cells that reside within the sand layer are cut off, as mentioned in section 4.3.2. This is done with the utility *snappyHexMesh* in which the coordinates of the sand layer are specified. The cobble layer is now effectively 'thinner' as the cobbles that were completely washed-in and covered with sand are also cut-off, see fig. 4.6.



(a) Detail of the top of the revetment of the S1T3 and S1T4 profiles.



(b) Detail of the top of the revetment of the S2T3 and S2T4 profiles.

Figure 4.5: Note that in both S1 and S2 test series the profile becomes steeper, the cobble layer of the revetment thinner and the crest is slightly elevated.

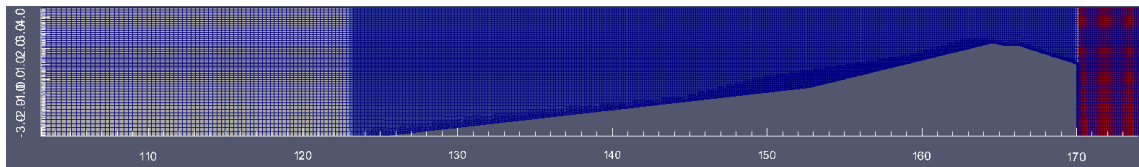


Figure 4.6: Overview of the numerical grid in Paraview with the sand slope cut out of the domain. Also note the finer meshes in and around the cobbles.

### Characteristics of the numerical cobbles

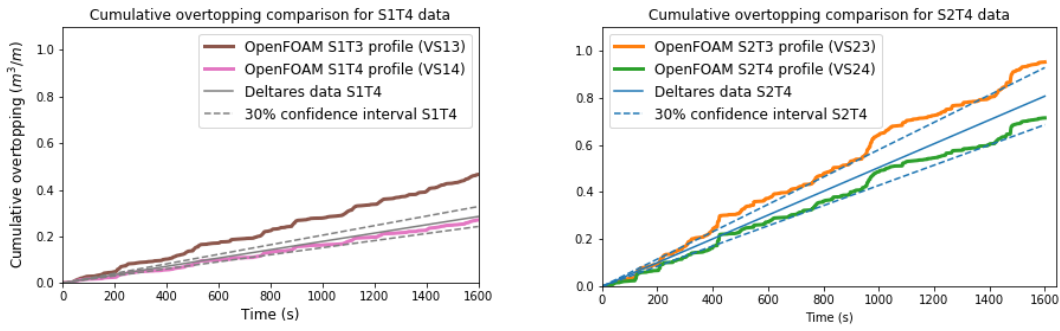
The cobble layer on top of the sand layer have been assigned the following characteristics  $d_{n,50} = 0.015m$  and a porosity  $n_p = 0.32$  for the S2T4 simulation and  $d_{n,50} = 0.015m$  and a porosity  $n_p = 0.32$  for the S1T4 simulation validation. The data is provided by Boskalis and is obtained from measurements of 10 soil samples taken on 10 locations on the revetment in cross shore direction after series S2. Boskalis hasn't provided any measurements of the porosity and diameter of the sand before or after the S1Tx tests.

### 4.5.3 Overtopping comparison

As discussed in section 4.5.2, for each of the S1T4 and S2T4 validations, two profile designs are used: the profile at the end of the SxT3 experiment and the profile measured at the end of the SxT4 experiment. All the simulations had a duration of 1600 seconds each.

Next to that, in the VS13 and VS14 simulations the finer mesh of case GB03 with 21693 cells have been used as a thicker cobble layer means that less overtopping is expected in the S1T3 and S1T4 experiments. A finer mesh is more capable of capturing the overtopping water. More information and a discussion on this choice can be found in section 4.4.1. For cases VS23 and VS24 the faster mesh of GB01 is used. This to enable acceptable clock times for the simulations to finish.

## Results



(a) The simulations under predict the overtopping discharge compared to the average specific overtopping discharge data of the S1T4 experiment. Input variables are a cobble porosity of  $n_p = 0.32$ , median cobble diameter of  $D_{n,50} = 14.6 \text{ mm}$  and a sand level of 0%.

(b) The simulations only slightly under predict the specific overtopping discharge by compared to the average specific overtopping discharge of the data of the S2T4 experiment. Cobble porosity is  $n_p = 0.32$ , median cobble diameter of  $D_{n,50} = 15.2 \text{ mm}$  and a sand level of 50% in the cobble layer.

Figure 4.7: Cumulative overtopping comparison of the numerical experiments and the data provided by Deltares.

In fig. 4.7 the average specific discharge data from the experiments S1T4 and S2T4 are compared to the numerical overtopping simulated in OpenFOAM. A total of four simulations have been completed. Two to reproduce the S1T4 experiment and two for the S2T4 experiment, see table 4.3. Expressed in relative differences:

- The average of the simulated specific overtopping discharges is calculated by adding  $1/3 \cdot q$  measured in VSx3 and  $2/3 \cdot q$  measured in VSx4.
- The average of specific overtopping discharges,  $q$ , simulated in case VS13 and VS14 is 16% larger when compared with those measured in the physical S1T4 experiment.
- The average of specific overtopping discharges,  $q$ , simulated in case VS23 and VS24 is 1% smaller when compared with those measured in the physical S2T4 experiment.

case	type	profile	Mesh	$q$ [l/m/s]
VS13	numerical	S1T3	GB03	0.29
VS14	numerical	S1T4	GB03	0.17
average	numerical	-	-	0.21
S1T4 data	physical	-	-	0.18
VS23	numerical	S2T3	GB01	0.59
VS24	numerical	S2T4	GB01	0.45
average	numerical	-	-	0.50
S2T4 data	physical	-	-	0.50

Table 4.3: The average specific discharge data from the experiments S1T4 and S2T4 are compared to the numerical simulations in OpenFOAM. A total of four simulations were conducted: two with the profile SxT3 profile and two with the SxT4 profile.

## 4.6 Sensitivity analysis

In this section the sensitivity of the numerical results is analysed for changes in the pseudo-random wave generator and the resistance coefficients of the Darcy-Forchheimer equation (see eq. 4.3).

### 4.6.1 Seed for pseudo-random wave generator

The aim of this section is to test whether the inbound irregular waves are a representative surface elevation realisation of the JONSWAP wave spectrum as used in the physical experiments and to test reproducibility.

The basic model for describing a moving surface elevation,  $\eta(t)$ , is the random-phase / amplitude model, in which the surface elevation is considered to be the sum of a large number of harmonic waves, each with a constant amplitude and a phase randomly chosen for each realisation of the time record with a large number of waves  $N$ .

Pseudo-random number generators work by performing some operation on a value. Each seed value will correspond to a sequence of generated values for a given random number generator. That is, if you provide the same seed for the pseudo-random wave generator twice, you get the same realisation of the surface elevation twice. To enable a comparison in a time-domain between simulations shorter than the full realisation of the time record one must use the same seed, i.e. relative overtopping volume per wave overtopping event between simulations can now be compared, instead of average overtopping discharge.

### Results

A figure of the trendlines of the specific cumulative overtopping volume of the simulations can be found in fig. 4.8. Expressed in relative differences:

- the specific overtopping discharge,  $q$ , simulated in case V05 increases by 4.2% when compared with the base case.

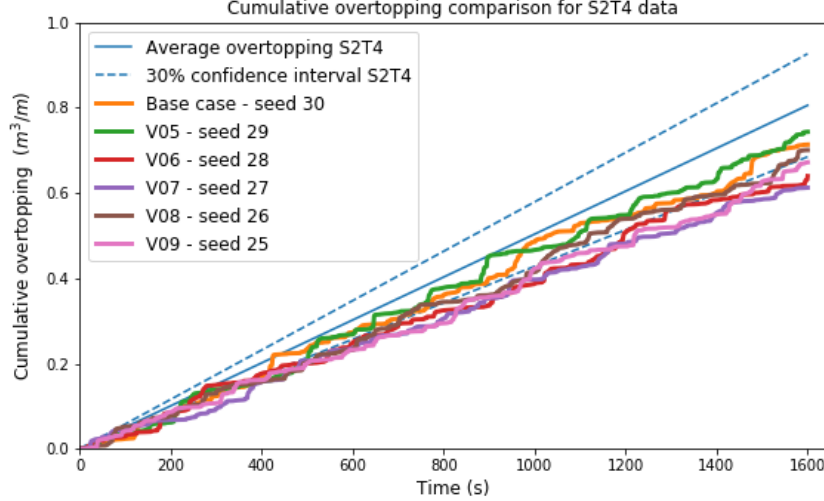


Figure 4.8: A total of 6 simulations reproducing the S2T4 experiment in which only the seed number for the random wave generator varies.

- the specific overtopping discharge,  $q$ , simulated in case V09 decreases by 5.8% compared with the base case.
- the maximum difference on the specific overtopping discharge,  $q$ , is 11%.

#### 4.6.2 Sensitivity in resistance coefficients of the Darcy-Forcheimer equation

In this section the sensitivity of amount of overtopping to the closure coefficients of the Darcy-Forcheimer equation (eq. 4.3) of the resistance term in the Navier-Stokes equation (eq. 4.1) is investigated. In literature two sets are most commonly used for flow in porous coastal structures forced by waves: Jacobsen et al., 2015 and Jensen et al., 2014, see table 4.4. See section 4.2.1 for more information.

Author	$\alpha$ [-]	$\beta$ [-]
Jacobsen et al., 2015	1000	1.1
Jensen et al., 2014	500	2

Table 4.4: The two most commonly used resistance closure coefficients for flow in porous breakwaters and coastal structures as a result of waves (Inigo J Losada et al. 2016).

### Results

Expressed in relative differences:

- With no sand washed-in to the revetment (S1T4 profile) the coefficients of Jensen et al. (2014) give a specific overtopping discharge,  $q$ , that decreases by 1.1% when compared to the simulation with the coefficients of Jacobsen et al. (2015).
- With 50% sand washed-in to the revetment (S2T4 profile), there is less than 1% difference in specific overtopping discharge,  $q$ , between the two simulations.

## 4.7 Variation in sand content in cobble layer

The aim of this section is to investigate the effect of (i) change in porosity of the cobble layer, and (ii) reduction of the effective cobble thickness of the S2T4 cobble profile and of a composite slope consisting of two straight sections. The numerical model's performance has been validated based on wave propagation and overtopping discharges in section 4.5. The sensitivities have been explored in section 4.6.

### 4.7.1 Description of the process of washing-in of sand

#### Physical processes

The washing-in of sand into the pores of the cobbles leads to:

- (i) A decrease of the overall porosity of the cobble layer as sand will partly fill up and potentially clog the spaces between the cobbles over the whole thickness and width of the cobble layer altering the flow of water in it.
- (ii) As sand falls and washes down through the cobble layer it will fill the pores from the bottom up, effectively decreasing the thickness of the revetment where flow is possible.

The initial porosity, cobble shape, cobble size, sand size and sand cohesion determines the rate at which process (i) and (ii) take place. See Appendix A for footage and more information on how the sand and cobbles were distributed over the height at various locations at the cobble revetment on the Maasvlakte II on the 21<sup>st</sup> of September 2018. A lot of spread is observed in the amount of sand clogging up pores in the field, as well as sand level within the cobble layer.

- (iii) As sand fills the pores and changes the porosity and hydraulic conductivity of the cobble layer by processes (i) and (ii), the initiation of motion, sediment transport and thus cross shore profile evolution under wave attack is altered.

#### Numerical schematisation of the processes

As the temporal and spatial distribution of the sand in the cobble profile is practically impossible to represent numerically, the following actions have been taken to numerically investigate the effect of the washing-in of sand on a cobble revetment. Instead of making an effort to exactly match these distributions:

- (i) The bounds of the influence of porosity of the cobble layer on average overtopping discharge,  $q$ , are calculated. The maximum and minimum values reported by Boskalis have been assigned for the whole numerical porous cobble layer.
- (ii) The bounds of the influence of the effective thickness of the cobble layer on the average overtopping discharge,  $q$ , have been simulated by:
  - (a) Decreasing the effective thickness of the cobble layer by increasing the level of the sand interface in the cobble S2T4 profile.
  - (b) Decreasing the effective thickness of the cobble layer of a composite profile consisting of two straight slopes by decreasing the level of the cobble layer.
- (iii) The effect of initiation of motion, sediment transport and profile development has not been simulated as the numerical model in it's current application has not been designed nor validated for this purpose.

### 4.7.2 Variation in porosity of cobble layer

In this section the influence of the porosity is investigated. The minimum value of porosity is equal to  $n_p = 0.29$  and a maximum of  $n_p = 0.42$ . Boskalis has measured sediment samples taken from the revetment after SxT5 series. These extreme values are now implemented in the cases with a profile of S1T4 which has no sand, and for the profile of S2T4 where 50% of the thickness of the cobbles has been washed-in with sand.

#### Results

The results of the four simulations can be found in table 4.5.

Case	profile	description	porosity [-]	$q$ [l/m/s]
S08	S1T4	no sand washed-in profile	0.29	0.13
S09	S1T4	no sand washed-in profile	0.42	0.11
S06	S2T4	50% sand washed-in profile	0.29	0.45
S07	S2T4	50% sand washed-in profile	0.42	0.42

Table 4.5: The results of simulations in which the porosity is varied between the minimum and maximum values of those measured in the physical experiments. Both the cross shore profile of the S1T4 and the S2T4 experiments have been simulated.

Expressed in relative differences:

- The specific overtopping discharge,  $q$ , simulated in case S08 increases by 19% when compared with case S09.
- the specific overtopping discharge,  $q$ , simulated in case S06 increases by 8.6% when compared with case S07.

### 4.7.3 Variation in sand level

#### S2T4 profile

Here the effective thickness of the cobble layer in each of the 3 simulations is changed by 50% relative to the cross-shore profile of case S2T4. This has been done by increasing the level of the sand-cobble interface. See fig 4.9 for an overview of the cross shore cobble and sand profiles.

#### Results

See table 4.6 for the results of the simulations.

Expressed in relative differences:

- The specific overtopping discharge,  $q$ , simulated in case S02 increases by 226% when compared with case S05.
- The specific overtopping discharge,  $q$ , simulated in case S04 decreases by 72% when compared with case S05.

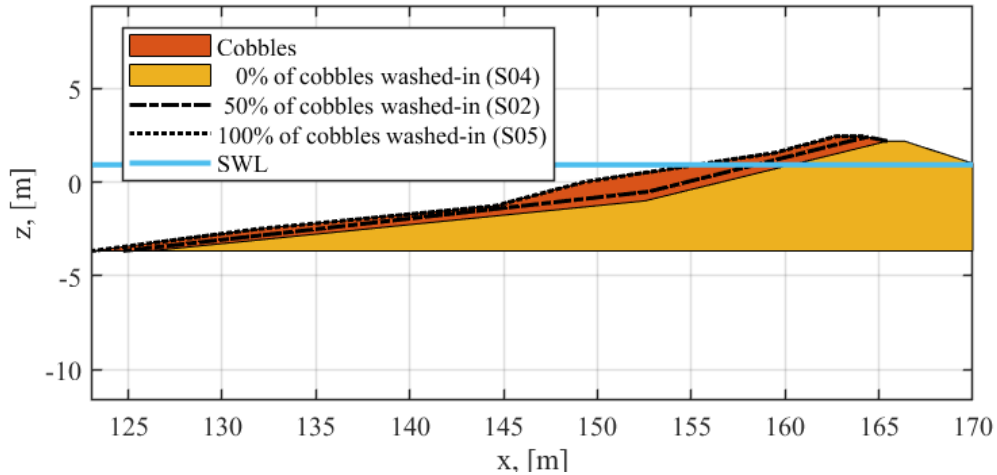


Figure 4.9: Overview of the sand levels within the cobble layer for each of the simulations.

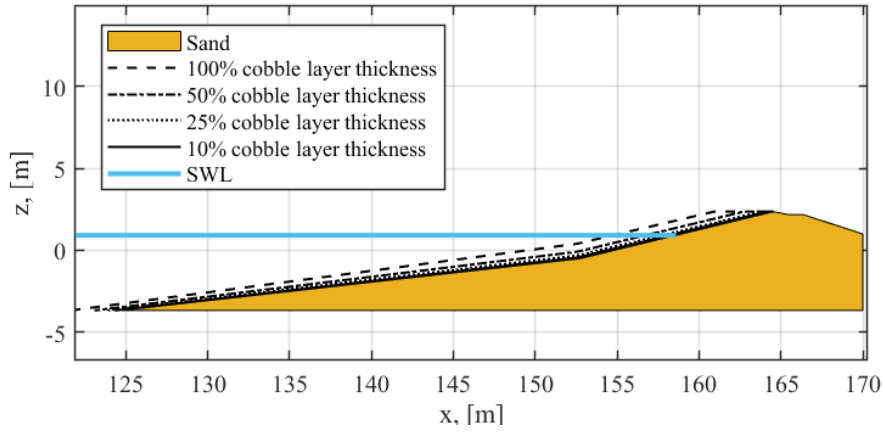
case	profile shape	description	porosity	$q$ [l/m/s]
S04	S2T4	0% of cobbles is washed-in	0.32	0.12
S02	S2T4	100% of cobbles is washed-in	0.32	1.37
S05	S2T4	50% of cobbles is washed-in	0.32	0.42

Table 4.6: The results of simulations in which the sand level in the cobble layer is varied. The cobble layer thickness is reduced by raising the internal sand level. The cross shore profile of the S2T4 experiment has been used.

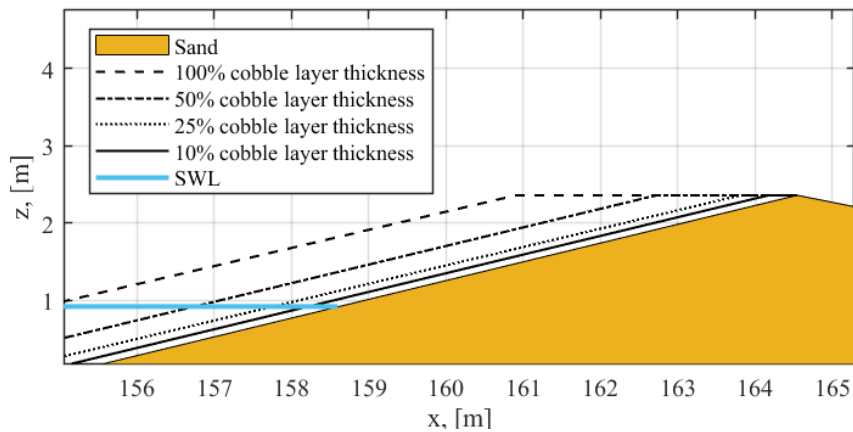
### Straight profile

The effect of the sand level in the cobble layer on the amount of overtopping is a central theme within this work. However, using the measured cross-sections from the experimental data of Deltares, it is difficult to create representative sand levels in the cobble profile due to its complex geometry. An effort is made to differentiate the effects of profile shape and washed-in sand level.

The following numerical experiments simulate waves breaking and overtopping on a composite slope existing of two straight sections with a porous cobble layer on top of an impermeable sand core. A total of five simulations with changing cobble layer thicknesses have been completed, each simulating a scenario with an increased amount of sand washed-in to the cobble revetment, i.e. a reduced effective thickness of the cobble layer. It is a similar approach, however, now the cobble layer is reduced in thickness at the water-cobble interface, instead of cutting away cobbles at the sand-cobble interface. This enables a fair comparison of the thickness of the cobble layer itself, as the absolute sand level and with that the impermeable layer of the revetment remains in the exact same location, see fig 4.10 for an overview and a detail.



(a) Overview of the cross shore profiles of all five simulations with incident waves similar to the S2T4 test.



(b) A detail of the top of the revetment. Note that the sand level does not change, as a higher vertical sand level would lead to a increased revetment height and thereby a decreased overtopping discharge. That is a unfair comparison when one wants to investigate the effect of the washed-in sand level, e.g. the effective thickness of the cobble layer.

Figure 4.10: An overview and detail of the composite slope consisting of a 1:9 and 1:4 slope.

## Results

See table 4.7 for the results of the simulations. Expressed in relative differences:

- When the effective thickness of the cobble layer is reduced from 100% to 10%, the specific overtopping discharge increases by 88%.

case	profile shape	cobble layer thickness [m]	relative cobble layer thickness [-]	$D_{n,50}$ [mm]	$q$ [l/m/s]
SS14	composite - two straight slopes	0.91	100%	15.2	0.47
SS10	composite - two straight slopes	0.45	50%	15.2	0.51
SS11	composite - two straight slopes	0.23	25%	15.2	0.73
SS12	composite - two straight slopes	0.09	10%	15.2	0.88
SS13	composite - two straight slopes	-	0%	15.2	1.73
SS14d	composite - two straight slopes	0.91	100%	152	0.35
SS10d	composite - two straight slopes	0.45	50%	152	0.40
SS11d	composite - two straight slopes	0.23	25%	152	0.68
SS12d	composite - two straight slopes	0.09	10%	152	0.81

Table 4.7: The results of simulations in which the thickness of the cobble layer is varied. The cobble layer thickness is reduced by decreasing the cobble height and keeping the cobble-sand interface in the same position. A composite slope consisting of two straight slopes has been used. Furthermore, in five simulations the median cobble diameter was  $D_{n,50} = 15mm$  and in four simulations  $D_{n,50} = 152mm$

# Chapter 5

## Analysis

The results of the numerical experiments are discussed in the following sections. First the overtopping validation simulations are dissected, after that the sensitivities are discussed. Then the results of the experiments in which the influence of porosity and sand level in the cobble layer are treated. Finally the application and dimensionless relations of the results are explored.

### 5.1 Overtopping validation

#### 5.1.1 Profile

The difference in numerical overtopping discharge of simulation VS13 (S1T3 profile) and VS14 (S1T4 profile) is larger than the difference in numerical discharges of simulation VS23 (S2T3 profile) and VS24 (S2T4 profile). That can be explained by the observations of M. v. Gent 2009 in his paper about the response of dynamic cobble structures to waves:

- The most dynamic response is expected for the most permeable structure and the average slope is steepest for the most permeable structure.
- If the pores between gravel/cobbles are filled with sand the response is less dynamic and as less erosion occurs below the waterline a lower crest is expected.
- The change in profile shape is largest at the start of the experiment, and moves towards an equilibrium as the experiments continues.

. In the S1 experiment series the cobble layer is thicker and the impermeable subsoil farther away from the cobble/water interface when compared with the S2 series. And indeed, the most dynamic response of the cobbles is observed in experiment S1T4. As a result, the crest height increases more, and more erosion occurs just below the waterline when exposed to waves. The numerical simulations of the overtopping discharges show the expected behaviour belonging to the profile change: the overtopping discharges decreases relatively more as the crest height increases relatively more.

It is unclear at what moment during the experiment in the Delta flume the largest part of the overtopping occurred. However, most likely at the start of the experiment as the crest height  $R_c$  is here at its lowest point. To capture this effect numerically the average of the simulated specific overtopping discharges are calculated by adding  $1/3 \cdot q$  measured in VSx3 and  $2/3 \cdot q$  measured in VSx4. Then they are compared to the experimental data, see table 4.3.

### 5.1.2 Performance of reproduction of S1T4 experiment

The bulk of the source of the over prediction of the average specific overtopping discharges in simulations VS13 and VS14 when compared with the the S1T4 experiment are expected to be related to the profile shape, explained in the subsection 5.1.1.

Other sources of uncertainty could be the total resistance of the flow in the porous media is underestimated. That can be the result of:

- an under estimation of the porosity,
- an under estimation of the  $D_{n,50}$ ,
- an over estimation of the KC number.

The cobbles and sand during the physical S1 experiment series have redeposited as the test has progressed through all the test stages time from SxT1 until SxT5. So, a certain form of spatial and temporal variation in cobble size and porosity can be expected in the cobble profile as sorting can take place during the physical experiments. In the numerical model however, an uniform value is assigned to  $D_{n,50}$  and porosity  $n_p$  for the whole cobble layer. The process of sorting can thus not take place numerically. The spatial difference could potentially be captured by measuring its distribution during the tests carefully and assign those to the characteristics of the numerical cobbles throughout the domain. However, unless a sediment transport model is implemented it will be impossible to capture the temporal change in porosity and sorting during the numerical simulations. This will remain a source of small uncertainty and can affect the results quantitatively.

An over estimation of the KC number could be the result of the fact that the KC number based on linear wave theory at the toe of the structure, where orbital velocity is an approximation of the maximum velocity in the top part of the cobble layer. When in fact, as waves break and run up the (turbulence) drag forces may become more important than the inertia terms on that location, while on other locations for example at the bottom of the revetment, drag does not play a role at all. No spatial or temporal distribution is possible in this numerical model. This uncertainty can effect the results quantitatively, but is expected to be orders smaller than the influence of for example profile shape.

### 5.1.3 Performance of reproduction of the S2T4 experiment

Simulations VS23 and VS24 reproduce the S2T4 experiment well: the numerical specific overtopping discharge and the specific overtopping discharge of the S2T4 experiment are almost alike.

In a similar fashion, it could be reasoned that in the VS23 and VS24 simulations the porosity and KC number are just overestimated, and the median grain size slightly underestimated. However, the uncertainty with respect to cross shore profile shape is larger than the uncertainty surrounding porosity and KC number.

### 5.1.4 Numerical error

In these simulations, the maximum mesh resolution was placed where wave breaking and overtopping occurs, as well as along the free surface throughout the entire domain. These regions had a uniform mesh grid with constant horizontal  $\Delta x$  and vertical  $\Delta y$  cell sizes. It is possible that increasing the mesh resolution in these regions could have improved the results from the simulations. However, this would have considerably increased the computational time of the simulations. As the comparisons between the simulations and measured data showed great agreement, it was decided not to modify the numerical mesh.

### 5.1.5 Conclusion

It can be concluded that compared with the experimental data the model is capable of simulating wave propagation, wave breaking, porous flow and overtopping for a cobble layer revetment on top of a sand core within a range of 16% for a cobble layer without sand washed into its profile, and within a range of 1% for a cobble layer that is washed-in with sand. The results have been obtained by averaging two simulations: one third of the discharge simulated with the cobble profile at the start of the physical experiment and two thirds of the discharge simulated with the profile of the cobbles measured after the physical experiment. In this way the reshaping of the cobbles during the experiment is approximated. Some uncertainties are related to this approach, but the results are great. The spatial and temporal change of the KC number, median cobble diameter and porosity are not captured in the simulations and remain another source of uncertainty.

## 5.2 Sensitivity analysis

### 5.2.1 Seed for pseudo-random wave generator

The difference between the different realisations is small. That is the result of the method used for discretisation of the frequency axis - it's called *cosineStretchedFrequencyAxis*. It produces a stretching of the frequency towards the peak of the spectrum and it greatly improves the statistical properties for the time series for the surface elevation; the derivation can be found in the appendix of Niels Gjøel Jacobsen 2017. Some seedings, such as seed 29, give 1 or 2 overtopping waves that contribute significantly to the overtopping quantities. Overtopping remains a non-linear process. In case overtopping discharges waves are small a handful of waves can strongly influence the result.

#### Conclusion

The influence of seeding is minimal. It can increase the numerical specific overtopping discharge,  $q$ , by 4% or decrease by 6% relative to the base case with seed number 30. The difference between the different realisations of the wave spectrum is small.

### 5.2.2 Sensitivity in resistance coefficients

The change as a result of the different resistance coefficients is minor. Remember: in profile S1T4 no sand is washed-in, in profile S2T4 half of the thickness is washed-in with sand. In simulations with no sand washed-in to the revetment, the difference in average specific discharge is not significantly larger.

#### Conclusion

The influence of the resistance coefficients on the average overtopping discharge,  $q$ , is  $\leq 1\%$ . The effects are not substantial compared to the influence of sand washing-in to the revetment or a change in porosity.

## 5.3 Variation in sand content in cobble layer

### 5.3.1 Variation in porosity

The closure coefficients  $a$  and  $b$  of the Darcy-Forchheimer flow resistance in a porous medium are described by the parameterisation by M. v. Gent 1995. As the porous medium in the physical experiments and the field contains particles of different sizes, several phenomena can appear at the same time at different places in the porous medium. Numerically these spatial differences in particle size are not captured, the uncertainties related to these topics, such as KC-number and  $D_{n,50}$  have already been discussed in section 5.1.2.

The overtopping is larger for a cobble revetment that has a lower porosity. That is in line with the expectations, as this behaviour is observed for many coastal structures such as breakwaters. The less water is able to infiltrate into the revetment, the more will overtop.

The relative difference in specific overtopping discharge is larger for the simulations with a thicker cobble revetment. As the cobble layer is relatively thicker in S1T4 profile, a change in porosity gives a larger change in the total friction resistance when compared with the simulations with the S2T4 profile. To put it simply: the more water is able to infiltrate into the pores of the cobbles over a wave period the larger the volume that can reside in the porous media, the smaller the overtopping rates. This behaviour is perfectly captured in the model. In section 5.4 the results of the different numerical simulations are compared to each other.

## Conclusion

The porosity has a significant influence on the overtopping rate in simulations. A larger effect is observed on a revetment with a thicker effective cobble layer as the total resistance force changes relatively more with the same increase in porosity. Uncertainties are related to the simplification of the characteristics of the porous medium. This is, however, inherently connected to the application of the Darcy-Forchheimer equation in the Navier-Stokes equation.

### 5.3.2 Variation in sand level

#### S2T4 profile

The specific overtopping discharge,  $q$ , increases considerably when the sand level within the cobble revetment increases. Less water can infiltrate into the pores as the cobble layer thickness becomes effectively thinner. This behaviour is in line with the expectations.

The difference between the S04 model run, where 0% of cobbles is washed-in with sand, and the VS14 model run is the cross shore profile shape. The berm at  $x=150$  m is thicker in the S04 model run and the cobble revetment slightly higher. The lower specific overtopping discharge can be attributed to these factors.

The overtopping simulated in the 100% washed-in cobble revetment (case S05) is most likely an overestimation. Recall that as the main aim of the model is to simulate flow in porous media no turbulence model is implemented. The resistance force on the flow of water as a result of waves is approximated through the Darcy-Forchheimer equations (see section 4.2.2). Case S05 lacks this porous layer, thus the model will overestimate the run-up and overtopping as the water rushing up the revetment does not experience

any significant friction. The surface roughness, boundary layer development, as well as momentum exchange over the water column as a result of turbulence is not accounted for explicitly. With the data provided and the scope of the research it was not feasible to implement a turbulence model.

It would be interesting to investigate what the relation is between an decreasing effective cobble thickness and the overtopping - in more gradual steps with the aim to parameterise the results. In section 5.3.2 the cross section is altered to a hypothetical situation where the cross shore profile is composed of two straight slopes. This way the cobble layer thickness, slope angle, crest height is evaluated with more accuracy.

### Composite slope

Here the effect on the overtopping is quantified by decreasing the effective cobble layer thickness,  $T_c = 0.92$  m, such that 100%, 50%, 25%, 10% and 0% of the layer thickness remains.

Again the model results show the expected behaviour: the specific overtopping discharge,  $q$ , increases considerably as the thickness of cobble revetment decreases. As waves break and run-up on the washed-in cobble layer revetment, sediment transport is expected. That wave action will bring sand that is covering the revetment quickly in suspension. A cobble profile that will remain completely covered and filled with sand over the course of a storm might therefore not be the most not realistic scenario. How deep the water will penetrate and remove sand from within the cobble profile and in what rate is an topic of on going discussion - and a research topic itself.

In case the effective thickness of the cobble layer is reduced from 100% ,  $T_c = 0.92$  m, to 10%,  $T_c = 0.09$  m, the specific overtopping discharge increases by 88%. This increase in overtopping discharge is physically more correct compared to the 100% washed-in sand case (case S02) simulated in the previous section as resistance of and infiltration in the porous medium is accounted for, as well as the consideration that some part of the sand in the top layer of the cobbles will wash out under high flow velocities. Overall the increase in average overtopping discharge is very significant when compared with the relative influence of uncertainties in section 4.6. As the model is very capable of simulating overtopping over a broad range of cobble thicknesses within a margin of 26%, these results are noteworthy.

In figure 5.1 the relation between the dimensionless overtopping rate, dimensionless cobble layer thickness for two nominal stone diameters can be observed. The larger the relative cobble layer thickness,  $T_c/H_{m0}$ , the lower the relative overtopping rate,  $q / (g H_{m0}^3)^{1/2}$ , up until a point that an further increase does not reduce the overtopping anymore. This point where 'the effective infiltration depth' is equal to 'effective cobble layer thickness', increases with increasing cobble diameter. That is explained by the fact that permeability (see eq. 4.3) is strongly dependent on the median stone diameter, and the infiltration depth is limited by both the period of a wave and permeability. More on infiltration, cobble size and scaling can be found in chapter 6.1.

### Conclusion

A decrease of the thickness of the cobble layer as a result of sand washing-in leads to an increased overtopping rate. The model most likely overestimates the overtopping rate for the simulations without cobble revetment as the model does not take into account bottom friction and bottom boundary layer effects during the up rush and down rush of waves in

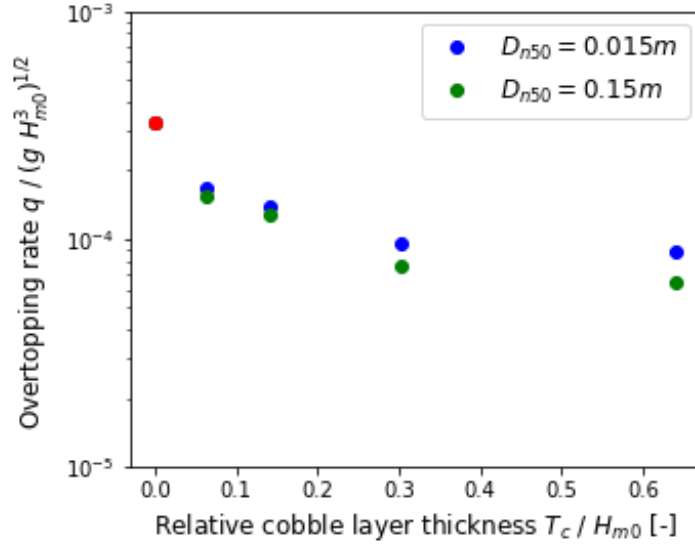


Figure 5.1: The relation between the dimensionless overtopping rate and dimensionless relative cobble layer thickness and median cobble diameter.

the swash zone as porous media lack. A plot of the relative overtopping rate plotted versus the relative cobble layer thickness shows an relationship which is as expected, though now finally quantified: the overtopping rate decreases in case the relative cobble layer thickness increases up until the point where 'the effective infiltration depth over a wave period' is equal to the 'effective cobble layer thickness'. This point increases with increasing stone diameter, as the permeability and thus infiltration increases.

## 5.4 Dimensionless relations of the results

### 5.4.1 Dimensionless relation

The parameters that have been investigated in this research, i.e. porosity and cobble layer thickness have shown to be very significant for the overtopping rate. Here an analysis of the parameter space is conducted. Porosity,  $n_p$ , is defined as the fraction of the volume of voids divided by the total volume and is dimensionless. The effective cobble layer thickness,  $T_c$ , is defined as the length in meters perpendicular to the sand interface and the surface of the cobble layer. Practically, this is measured halfway between the mean water surface elevation and crest elevation,  $R_c$ .

In fig. 5.2a the crest elevation,  $R_c/H_{m0}$ , is modified to by replacing,  $R_c$  with porosity,  $n_p$ , times effective thickness of the cobble layer,  $T_c$  resulting in the dimensionless quantity:

$$\frac{n_p \cdot T_c}{H_{m0}} \quad (5.1)$$

In figure 5.2b the results of the crest height layer thickness parameter are plotted against the relative overtopping rate. Relative crest elevation,  $R_c/H_{m0}$ , is multiplied by the  $T_c/H_{m0}$  to obtain:

$$\frac{T_c \cdot R_c}{H_{m0}^2} \quad (5.2)$$

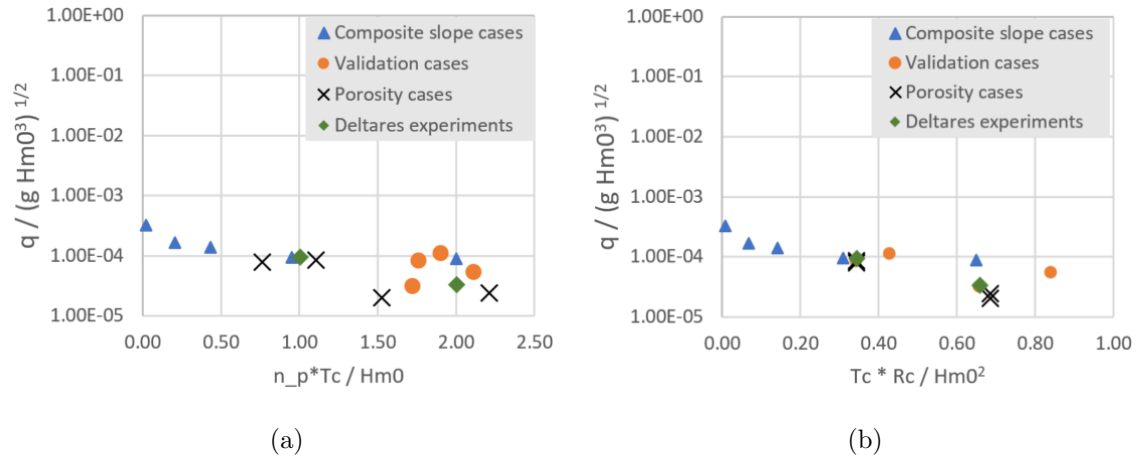


Figure 5.2: For both figures great correlation is observed. However, in figure 5.2a some degree of scatter is observed around  $n_p \cdot T_c / Hm0 \approx 2$  as the influence of the crest height misses.

Both figures show relations between the porosity and relative overtopping rate and the influence of the thickness on the relative overtopping rate within the parameter space that is investigated.

The relative crest height remains, however, an very important parameter. Plotting the relative overtopping rate with  $n_p \cdot T_c / Hm0$  (fig. 5.2a) is proven to be useful in this work, but for application in equation 5.7 where  $R_c$  is already represented. In a similar fashion it can be argued that in fig. 5.2b the significant porosity parameter is lacking.

The developed theory is that a part of the volume over every wave run-up tongue is sinking into the pores of the cobble revetment and does not overtop. The wave overtopping volume of each overtopping wave is thus reduced by the total volume of the pores that can be infiltrated over a cycle of a wave. This is a similar approach as Steeg, Breteler, and Provoost 2016. The total pore volume per meter width  $V_{pores} [m^3/m]$  above the water line can be calculated by:

$$V_{pores} = n_p \cdot L_{slope} \cdot T_c = n_p \cdot R_c \cdot \sqrt{1 + \cot^2 \alpha} \cdot T_c \quad (5.3)$$

With  $\alpha$  being the mean slope of the revetment above the mean water surface water elevation and  $T_c \leq T_{c,maxeffective} \approx L_{infiltration}$ . As the total pore volume of the layer can only be filled with water when the maximum infiltration depth over a wave period is larger than the effective thickness of the cobble layer. Pores that lay deeper than the infiltration depth  $L_{infiltration}$  of water over a wave period will not be reached by the water within a wave period and will therefore not contribute in reducing overtopping volumes directly. More on the relation between infiltration and cobble size can be found in section 6.1.

The dimensionless pore volume number is obtained by dividing the pore volume per meter width by the spectral wave height squared:

$$\frac{n_p \cdot R_c \cdot \sqrt{1 + \cot^2 \alpha} \cdot T_c}{H_{m0}^2} \quad (5.4)$$

where

$$0.29 \leq n_p \leq 0.42 \text{ and } T_c \leq L_{infiltration} \quad (5.5)$$

When using equation 5.3 the subsequent assumptions are made:

- The pores are empty at the moment the wave run-up tongue is above the cobble layer.
- The pores are hydraulically connected.
- The effective thickness of the cobble layer is the thickness smaller than or equal to the infiltration depth over a wave period.

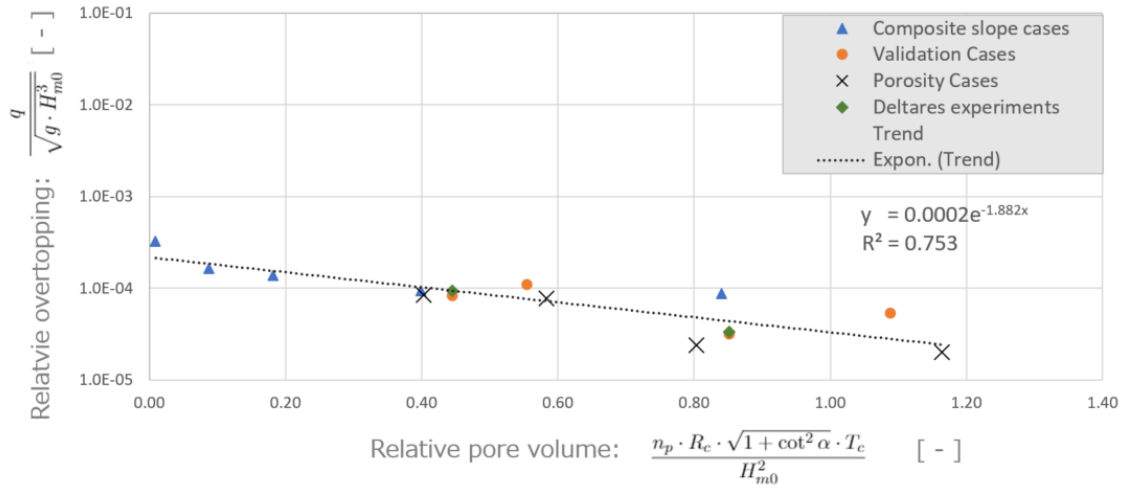


Figure 5.3: The relation between dimensionless pore volume number is set out against the relative overtopping rate for the results of the numerical experiments, as well as the physical experiments.

A clear correlation is observed when looking at figure 5.3. However, one must take care with extrapolating and increase the cobble layer thickness for scale tests on this scale. For example, the composite slope case with the thickest cobble layer and with the largest relative pore volume is plotted above the trend line as the relative overtopping rate is quite large. That can be explained by the fact that the thickness of the revetment is larger than the infiltration length  $L_{infiltration}$ , as can be observed in figure 5.1.

The relative pore volume number of the Porosity and Deltares cases is comparably large as a result of an increased crest height and large porosity, but it is associated with smaller relative overtopping as the pores are more easily infiltrated with water.

Though, it is noted that as a result of the stability number scaling to determine the the cobble size in the Deltares experiments, the infiltration depth isn't scaled correctly, see chapter 6.1 for an discussion.

## Conclusion

The dimensionless relation captures all the parameters investigated in this research and can be represented by an exponential relationship within the boundaries of the parameters used in this work. Care must be taken with increasing the cobble layer thickness, as the infiltration depth of the water is limited on model scale. The OpenFOAM model could be used to simulate more scenarios with the goal to increase the certainty in the relations and better the regression fit.

### 5.4.2 EurOtop (2018)

The EurOtop manual (2018) is often used to predict overtopping discharges for coastal structures with formulae fitted on the data of the extensive data base dubbed CLASH. A comparison is made with the general formula for the mean overtopping discharge on a sloping embankment and a relation for the determination of the roughness factor is proposed.

The general formula for the mean overtopping discharge on a slope (dike, levee, embankment) is given by the mean value approach (EurOtop 2018):

$$\frac{q}{\sqrt{g \cdot H_{m0}^3}} = \frac{0.023}{\sqrt{\tan \alpha}} \gamma_b \cdot \xi_{m-1,0} \cdot \exp \left[ - \left( 2.7 \frac{R_c}{\xi_{m-1,0} \cdot H_{m0} \cdot \gamma_b \cdot \gamma_f \cdot \gamma_\beta \cdot \gamma_\eta} \right)^{1.3} \right] \quad (5.6)$$

$\gamma_f$  is the influence factor for roughness on a slope,  $\gamma_\beta$  is the influence factor to account for oblique waves,  $\gamma_b$  is the influence factor for a berm,  $\gamma_\eta$  is the influence factor for a wall at the end of a slope,  $\xi_{m-1,0}$  is the breaker parameter (Iribarren number), and  $R_c$  the crest elevation.

In the case on hand  $\gamma_b$ ,  $\gamma_\beta$ ,  $\gamma_\eta$  are all equal to 1. The roughness factor  $\gamma_f$  typically accounts for grass, asphalt or impermeable block revetment systems. The development of new revetment types with the ability to absorb some of the up rushing water demanded a new way to define the roughness coefficient other than only the heights of the elements giving 'roughness'. The influence factor of porous block systems has been parameterised in a study by Steeg, Breteler, and Provoost 2016 as a relation of the dimensionless pore volume per square meter and influence factor  $\gamma_f$ . The infiltration of water into the pores of the cobbles is a similar process when compared with the infiltration into the channels of the blocks during wave run-up.

type of revetment		Hillblock	Cobble
author		van Steeg (2016)	Zaalberg (2019)
slope (average)	$\cot \alpha$	3	5.5
porous volume	m <sup>3</sup> /m <sup>2</sup>	0.034 - 0.058	0.030 - 0.40
breaker parameter	$\xi_{m-1,0}$ (-)	1.39 - 2.94	0.95
influence factor roughness	$\gamma_f$ (-)	0.69 - 0.81	0.62 - 0.75
influence factor berm	$\gamma_b$ (-)	1	1
influence factor angle of incidence	$\gamma_\beta$ (-)	1	1

Table 5.1: Comparison of the parameter range of the study of Steeg, Breteler, and Provoost 2016 into the effect of porosity on the influence factor  $\gamma_f$  of equation 5.6 and the numerical experiments conducted by Zaalberg 2019 and the experiments conducted in the Delta Flume 2007.

The  $\gamma_f$  can be determined by comparing a fit through the reference curve, i.e. the overtopping formula equation 5.6, with all influence factors equal to 1.0 except for the roughness factor. The roughness factor  $\gamma_f$  can now obtained by rewriting equation 5.6 to:

$$\gamma_f = \frac{2.7 \cdot R_c}{\xi_{m-1,0} \cdot H_{m0} \left( -\ln \left( \frac{\frac{q}{\sqrt{g \cdot H_{m0}^3}}}{\frac{0.023}{\sqrt{\tan \alpha}} \gamma_b \cdot \xi_{m-1,0}} \right) \right)^{\frac{1}{1.3}}} \quad (5.7)$$

The roughness factors are plotted against the dimensionless quantity pore volume per area in figure 5.4.

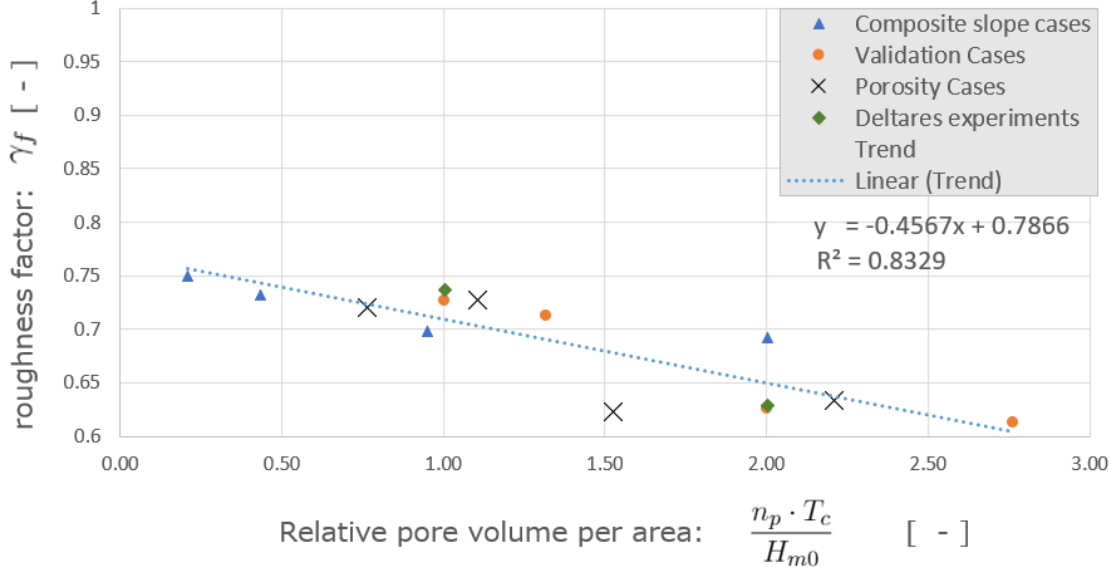


Figure 5.4: The relation between the relative pore volume per area and roughness factor.

Now the roughness coefficient can be related to the dimensionless pore volume area by regression through the data points. This is an approximation for the experimental results within the parameter space of this work (see 5.1). The equation is as follows:

$$\gamma_f = 0.77 - 0.46 \cdot \frac{n_p \cdot T_c}{H_{m0}} \quad (5.8)$$

for:

$$0.21 \leq \frac{n_p \cdot T_c}{H_{m0}} \leq 2.77 \quad (5.9)$$

and

$$T_c \leq L_{infiltration} \quad (5.10)$$

The remarks that have been made in section 5.4.1 apply here as well. Spread in roughness factor,  $\gamma_f$ , can be observed around  $1.5 \leq n_p \cdot T_c / H_{m0} \leq 2.0$ . That can be explained by the fact that the extra cobble layer thickness of the composite slope case does not contribute much to decrease overtopping as it is almost equal to the infiltration depth of water. Whereas an increase in porosity for the porosity case increases the infiltration rate, making the total pore volume of the cobble layer more accessible and thereby decreasing overtopping significantly.

Section 6.2 is referred to for a discussion on the sensitivity of the EurOtop 2018 formula by Van der Meer et al. 2018 for overtopping (equation 5.6) on gentle slopes to the

breaker parameter,  $\xi_{m-1,0}$ .

More research and more (numerical) experiments need to be conducted to be able to increase certainty in predicting the roughness factor as a function of the relative pore volume per area. Challenges that need to be solved include an easy and reliable method to estimate the infiltration depth over an wave cycle, as this is a source of spread in the relation. Moreover, the influence of changing incoming wave height, wave period, crest height, water level as well as revetment slope needs to be scrutinised and quantified before this dimensionless relation has gained sufficient reliability to use it in practical applications for contractors and consultants.

# Chapter 6

## Discussion

The research question was stated as follows:

*What is the influence of a decrease in porosity and cobble layer thickness on the overtopping as a result of sand washing-in to a cobble revetment?*

OpenFOAM® allowed the author to simulate a large amount of scenarios in which the influence of cross-shore profile shape, cobble porosity, cobble diameter and layer thickness on the overtopping were examined, quantified and analysed. Four validation runs and six simulations to map the sensitivity are compared with data from two physical experiments. It proved the correct working of the model. Then, another 16 simulations with the cobble revetment featuring a variety of porosity, thickness and shape have been completed. The model results show interesting relations when compared with each other. The relation is best captured in a new dimensionless quantity proposed by the author:  $n_p \cdot R_c \cdot \sqrt{1 + \cot^2 \alpha} \cdot T_c / H_{m0}^2$  which has an logarithmic relationship with the dimensionless overtopping rate  $q / (g \cdot H_{m0}^3)^{0.5}$  for the parameter space considered in this research.

In the next sections some essential aspects of the results are discussed and put into context. It's examined whether they corroborate, extend, refine or conflict with previous findings and studies, if they exist.

### 6.1 Infiltration depth and scaling

The median cobble diameter used in the experiments conducted in the Delta flume and numerical experiments have been scaled using stability number. However, flow resistance and permeability does not scale linearly with a decrease in cobble diameter - like the stability number and cobble diameter do. The implications for the infiltration rate of water in to the cobble layer are explained in the next section.

Recall that in figure 5.1 the relation between the dimensionless overtopping rate, dimensionless relative cobble layer thickness and nominal stone diameter was shown. The larger the relative cobble layer thickness,  $T_c / H_{m0}$ , the lower the relative overtopping rate,  $q / (g H_{m0}^3)^{1/2}$ , up until a point that an further increase does not reduce the overtopping anymore. This point where 'the effective infiltration depth' is equal to 'effective cobble layer thickness', increases with a larger cobble diameter. That is explained by the fact that permeability (see eq. 4.3) is strongly dependent on the median stone diameter, and the infiltration depth is limited by both the period of a wave and permeability.

However, the cobble size used in the Deltares experiments have been determined by applying the stability number as scaling law:

$$\frac{H_{m0}}{\Delta D_{n50}} \Rightarrow H_{m0} \sim \frac{1}{D_{n50}} \quad (6.1)$$

Remember that the flow resistance term in equation 4.1 as a result of flow through porous media is determined by the Darcy-Forcheimer equation:

$$\mathbf{F}_p = \rho a \mathbf{u} + \rho b \|\mathbf{u}\|_2 \mathbf{u} \quad (6.2)$$

and that the closure coefficients  $a$  and  $b$  are evaluated based on the parameterisation by M. v. Gent 1995:

$$a = \alpha \frac{(1 - n_p)^2}{n_p^3} \frac{v}{D_{n,50}^2} \Rightarrow a \sim \frac{1}{D_{n,50}^2} \quad (6.3)$$

$$b = \beta \left(1 + \frac{7.5}{KC}\right) \frac{1 - n}{n^3} \frac{1}{D_{n,50}^2} \Rightarrow b \sim \frac{1}{D_{n,50}^2} \quad (6.4)$$

The median cobble diameter is scaled linearly, using the stability number as scaling law, to ensure a similar morphological behaviour of the cobble layer in the model tests. The closure coefficients of the resistance force determining the flow velocity in the porous medium, however, scales quadratically. This means that the change in resistance force for flow in the porous medium also scales quadratically (see figure 6.1).

Moreover, as a result of this scaling effect, a change in porosity leads to a much higher difference in flow resistance for the model scale median grain diameter,  $D_{n,50}$ , used in the Deltares experiments when compared with prototype scale  $D_{n,50}$  (see figure 6.1). Thus, the experiments conducted in the Delta Flume and numerical experiments underestimate the infiltration rate, and as a consequence overestimate overtopping compared to prototype scale.

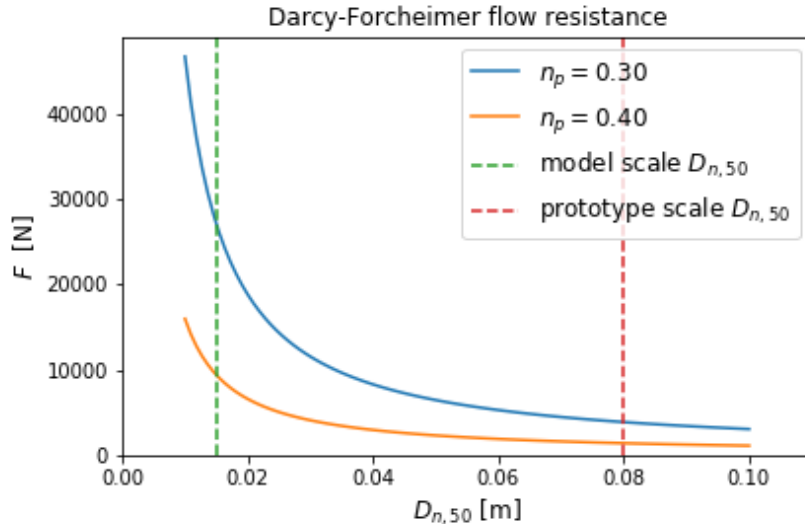


Figure 6.1: The relation between the flow resistance in the porous medium approximated by Darcy-Forcheimer and cobble diameter size for porosity  $n_p = 0.30$  and  $n_p = 0.40$ .

## 6.2 Profile shape

The cross shore profile shape of the cobble layer has shown to significantly influence the overtopping discharge. Key parameters include cobble layer thickness, crest height and slope.

One of the drawbacks of the numerical model used in this study is that the morphodynamic developments of the cobble layer and sand is not captured *during* the simulations. No effort was made to include morphological developments of the cobble and sand layer in the framework, as a major overhaul of the numerical model is needed:

- (i) to account for transport of sand and cobble particles,
- (ii) as a consequence of the transport of the particles, a modification of the mesh for every time step is needed as the location of the porous medium changes, and
- (iii) as a turbulence model needs to be implemented to correctly model important processes for sediment transport such as acceleration effects and turbulence induced by wave breaking.

One study by Niels G Jacobsen et al. 2018 includes a sediment transport formula in the OpenFOAM framework and is able to model the movement of sand in a filter. Here, however, the sand interface is modelled as an impermeable boundary layer. Thus the boundaries of the mesh are changed, not the location of the porous media within the mesh boundaries.

In this dissertation fixed profiles from both measured and hypothetical cross sections resulted in a relation between the dimensionless overtopping rate and relative pore volume. Encouraged by the results, a similar relation was defined in which the roughness factor,  $\gamma_f$ , of the EurOtop 2018 formula for mean overtopping discharge for dikes and levees can be estimated as a function of the relative pore volume per area. This looks like a elegant procedure to omit the cumbersome procedure to account for composite slopes and berms and all in the formula in EurOtop 2018.

However one must be cautious, the EurOtop 2018 formula by Van der Meer et al. 2018 for overtopping (equation 5.6) on gentle slopes is sensitive to the breaker parameter,  $\xi_{m-1,0}$ . The breaker parameter,  $\xi_{m-1,0}$ , itself is dependent on the slope of the cobble layer - which changes when exposed to waves. Steeg, Breteler, and Provoost 2016 didn't have to deal with this issue, as the porous concrete blocks were fixed.

In case of large rocks the armour layer will form a steep slope resulting in a overtopping formula for "non-breaking" waves. Here, the overtopping rate is insensitive for fluctuations in the slope. This means that a composite slope and even a, not too long, berm leads to the same overtopping discharge as for a simple straight rubble mound slope. Storms will reshape the berm to a certain extent and may even become a structure with a fully reshaped S-profile. Such a profile has then a gentle 1:4 or 1:5 slope just below the water level and steep upper and lower slopes, see Sigurdarson and Van der Meer 2011.

As a consequence of the relatively small rocks the steepest parts of the revetments in this study feature a slope of 1:4, and the lower part below the water level is closer to 1:9. Also, the revetment has an impermeable core in contrast with the breakwaters tested by Sigurdarson and Van der Meer 2011. So, this formula and approach is not particularly useful in this case.

The approach to predict the breaker parameter accurately to either find the relation between the characteristics of the cobble (and sand) layer, the characteristics of the inbound waves and the resulting profile shape. Several studies have been conducted to this relation, for example M. v. Gent 2009; López De San Román Blanco 2003; Pedrozo-Acuña et al. 2007; She, Horn, and Canning 2007. However, it was observed that a complex balance of processes is responsible for the profile evolution of coarse-grained beaches with no single dominant process. It is thus not expected that this relation is easy to define.

The other approach is the approach used in this work - measure profile development as a result of physical experiments or data from the field and calculate the breaker parameter from those values. That means that is more difficult to estimate overtopping discharges upfront, in case no experiments or field observations exist.

### 6.3 Turbulence

No separate turbulence model is used for the simulations. The Darcy–Forchheimer equation was introduced to the Navier–Stokes equations as a closure model for handling the porous media resistance force which cannot be resolved directly in the model. If the resistance coefficients,  $\alpha$  and  $\beta$ , are found from measurements they already include the effect of turbulence (Jensen, Niels Gjørl Jacobsen, and Christensen 2014). The reasoning being that the properties of the dissipative permeable cobble layer were the main interest of this work. However, next to the turbulence produced by the porous layer that is included in the resistance coefficients, wave breaking does play a role and is a source of turbulence production outside the porous layer. But adding a turbulence model to the numerical framework, one should also modify the resistance coefficients to prevent double dissipation of the motion as a result of turbulence.

Bottom friction as well as bottom boundary layer development as a result of turbulent motion is thus not accounted for explicitly. With the data provided and the scope of the research it was not feasible to implement a turbulence model. Determining the roughness coefficients of the cobble layer surface with sand washed-in, testing boundary layer development over the cycles of a wave period and measuring turbulence levels takes a whole different approach. It requires experimental data of flow velocities, surface elevations and run-up and overtopping values with extremely high temporal and spatial resolution.

For a detailed account on the numerical validation of run-up and swash hydrodynamics on permeable and impermeable fixed straight slopes in a Reynolds Averaging Navier Stokes (RANS) model is referred to Arana 2017. In the work of Brown 2017 a thorough comparison of turbulence models is made for application in surf zone dynamics. His results showed that all of the tested variables were in a high degree sensitive to the choice of turbulence model. In addition, including turbulence models increases the computational costs remarkably as higher mesh resolutions and shorter time steps are needed. More information and application of numerical models on water waves interacting with porous coastal structures can be found in Inigo J Losada et al. 2016.

Jensen, Niels Gjørl Jacobsen, and Christensen 2014; Vanneste and Troch 2015 argue that for an engineering approach the actual levels of turbulence are of limited interest, in this approach the turbulence can also be captured in the Darcy-Forchheimer equations. In addition, as the comparisons between the simulations in this work and measured data also showed great agreement, it was decided not to include a turbulence model.

# Chapter 7

## Conclusions

This chapter deals with the conclusions that can be drawn from this research. First each of the sub-questions will be evaluated, then the main research question will be answered.

### 7.1 Sub-questions

- (i) What is the most suitable numerical model for simulating overtopping on a cobble revetment?

Through a literature study the (dis)advantages of the existing numerical models capable of solving the Navier-Stokes equations have been reviewed. Various flavours and types exist, however, few are depth resolving and capable of modelling flow in porous media. Moreover, the model needed to be able to successfully generate and absorb irregular waves during long simulation times. Next to these theoretical constraints, practical limitations have also been taken into consideration, for example computational availability and software licensing costs. OpenFOAM® with the waves2foam toolbox was identified as the most suitable numerical model for simulating overtopping on a cobble revetment.

- (ii) What experiments are most suitable to reproduce and thereby validate the numerical model outcomes with?

A data set has been obtained for the validation of the results numerical model. It comprises the physical experiments conducted in the Delta Flume completed during the design phase of the Maasvlakte II revetment. This data set contained 30 experiments, of which two experiments proved to be most suitable: test S1T4 and the S2T4. In the S1 experiment series no sand was washed-in the cobble layer, in the S2 experiment 50% of the cobble layer thickness had been washed-in with sand. Test conditions exposed the cobble layer to a water surface elevation of  $h = 0.92 \text{ m} + \text{NAP}$  with JONSWAP wave spectrum featuring a peak period of  $T_p = 5.72 \text{ s}$ , a spectral wave height,  $H_{m0} = 1.42$  and a peak enhancement factor of  $\gamma_f = 2.2$  (all on model scale). Deltares provided data of: the revetment characteristics, profile measurements, wave flume dimensions, characteristic inbound wave statistics as well as average overtopping discharge for each of the experiments. Only from the S2T4 experiment the raw surface elevation over time measurements have been made available by Deltares; no paddle velocity signal, nor overtopping volumes over time were found.

- (iii) How well can the numerical model reproduce the experiments and what are its sensitivities?

The numerical wave flume has been setup and successfully reproduces the inbound waves, cross shore profile, cobble characteristics and sand content of the physical experiment. The model is capable of simulating wave propagation, wave breaking and porous flow. The mesh is an integral part of the numerical solution and must satisfy certain criteria to ensure a valid approximation of the solution. A thorough mesh study has been conducted.

The specific overtopping discharge for the cobble layer on top of an impermeable sand core is estimated within 26% error for a cobble layer without sand washed-in to its profile (S1T4 test), and within an error of 1% for a cobble layer that is washed-in with sand (S2T4 test). As the cobbles cannot move in the numerical model, the numerical overtopping discharges are obtained by averaging the results of the simulations using the cross shore profile measured at the start and a profile measured the end of the S1T4 and S2T4 test.

The dynamic behaviour of the cobbles during the physical tests is cumbersome to approximate in a static numerical profile and remains the largest source of uncertainty in the validation as can be seen by the numerical experiments aiming to reproduce the S1T4 experiment.

To account for the transport of rocks and/or sand it would be necessary to include a relation describing transport, but also a turbulence model. Four reasons why a turbulence model was not included in this work were: (i) in literature it was found that model outcomes were very sensitive to the choice of turbulence model and parameter input, (ii) it requires experimental data of flow velocities over the water column, surface elevations, run-up and overtopping values with extremely high temporal and spatial resolution for validation - something that wasn't available, (iii) for an engineering approach the actual levels of turbulence are of limited interest - with this approach the turbulence can also be captured in the Darcy-Forcheimer equations, and (iv) comparisons between the simulation results and the physical model data showed great agreement.

The spatial and temporal change of the KC number, median cobble diameter and porosity are not captured in the simulations and remain an other source of uncertainty. These parameters are related to the simplification of the characteristics of the porous medium. This is, however, inherently connected to the application of the Darcy-Forcheimer equation in the Navier-Stokes equation. Other sensitivities of the model have been explored as well, such as the effect of seed selection and the influence of the resistance coefficients for the Darcy-Forcheimer equation. These effects were not substantial.

## 7.2 Research question

The research question is formulated as follows:

What is the influence of a decrease in porosity and cobble layer thickness on the overtopping as a result of sand washing-in to a cobble revetment?

Another 16 simulations have been completed in the validated numerical wave flume to quantify the maximum influence a change in porosity, sand level and profile shape can have. The influence of washing-in of sand on a cobble revetment is quantified by simulating the following scenarios:

- (i) the porosity of the cobble layer is varied, in which

- (a) 2 simulations feature the S1T4 cross shore profile.
  - (b) 2 simulation feature the S2T4 cross shore profile.
- (ii) the effective cobble thickness is varied, in which
- (a) 3 simulations feature the S2T4 cross shore profile, and
  - (b) 9 simulations feature a composite slope consisting of two straight sections.

Both a decrease in porosity, and a decrease in cobble layer thickness lead to a reduction of pore volume in the cobble layer, and as a result, an increase in overtopping discharge.

### Relative pore volume number

The idea is that a part of the volume of the overtopping wave run-up tongue is sinking into the pores of the cobble revetment and does not overtop. The wave overtopping volume is thus reduced by the total volume of the pores that can be infiltrated over a cycle of a wave. This is a somewhat similar approach as Steeg, Breteler, and Provoost 2016 used for concrete blocks with channels in it, capable of absorbing part of the water rushing up and down the revetment. This theory can be captured in a new dimensionless number which accounts for the total volume of pores between the cobbles above the mean waterline normalised by the spectral wave height squared. It is called the relative pore volume number:

$$\frac{n_p \cdot R_c \cdot \sqrt{1 + \cot^2 \alpha} \cdot T_c}{H_{m0}^2}$$

In which  $n_p$  is the porosity,  $R_c$  the crest height,  $\alpha$  the slope of the revetment above the waterline,  $T_c$  the effective thickness of the cobble layer above the water line and  $H_{m0}$  the spectral wave height.

When the relative pore volume number is set out against the relative overtopping rate,  $q / (g H_{m0}^3)^{1/2}$ , it shows a clear logarithmic correlation for the parameter space covered in this research. The larger the relative pore volume number, the smaller the relative overtopping rate.

Some remarks have to be made. The effective thickness,  $T_c$ , is limited by the infiltration rate of the water in the numerical model experiments, i.e. pores that lay too deep cannot be filled with water during a wave cycle as the resistance force is fairly high for small cobble diameters. The median cobble diameter that was used in the (model) scale experiments in the Delta Flume, as well as numerically, have been determined by using stability number as scaling law, thus linearly. This was done to ensure the morphodynamic behaviour of the cobble layer on model scale is similar to its behaviour on prototype scale. The infiltration rate, however, does not scale linearly with the median cobble diameter, this scaling effect means that with the model scale outcomes the infiltration rate on prototype scale will be underestimated and the overtopping rate, thus, overestimated.

### EurOtop 2018

The volume of pores per area above the mean water level is thus related to a reduction in overtopping volumes. The influence factor for roughness,  $\gamma_f$ , of the general formula for predicting the mean overtopping discharge on a slope (equation 5.6) in EurOtop 2018 by Van der Meer et al. 2018 is modified by comparing a fit through the reference curve of all

the numerical and physical experiments. The roughness factor,  $\gamma_f$ , can now be calculated as a function of the relative pore volume per area:

$$\gamma_f = 0.77 - 0.46 \cdot \frac{n_p \cdot T_c}{H_{m0}}$$

for:

$$0.21 \leq \frac{n_p \cdot T_c}{H_{m0}} \leq 2.77$$

and

$$T_c \leq L_{infiltration}$$

However, when using this relation one must be cautious, the EurOtop 2018 formula for overtopping (equation 5.6) on gentle slopes is sensitive to the breaker parameter,  $\xi_{m-1,0}$ . The breaker parameter,  $\xi_{m-1,0}$ , itself is dependent on the slope of the cobble layer - which in dissertation is fixed, but in reality changes when exposed to waves. The formula used for reshaping (berm) breakwaters of Sigurdarson and Van der Meer 2011 is not applicable as it accounts for large breaker parameters,  $\xi_{m-1,0}$  as a result of the large rocks forming a steep slope. The solution is to determine the breaker parameter by either finding the relation between the characteristics of the cobble (and sand) layer, the characteristics of the inbound waves and the resulting profile shape, or measure profile development as a result of physical experiments or data from the field.

## Chapter 8

# Recommendations

Suggestions for further research include:

- The numerical experiments are validated with data with a fairly low spatial and temporal resolution. To increase understanding in the numerical model, it is suggested to collect overtopping data of physical experiments with high spatial and temporal resolution. In these experiments it would be valuable to quantify the influence of median cobble diameter of the cobbles, sand content, crest height, amongst many. The measurement should include the wave paddle velocity signal, surface elevation over time of numerous wave gauges along the length of the flume, run up heights, swash velocities, overtopping volumes over time and cross shore profile measurements. This way wave-to-wave comparisons in the time domain can be made, instead of in a statistical framework as used in this work. This method facilitates a better evaluation of each of the relevant processes that are modelled. Furthermore, for an equivalent computational cost, mesh resolutions can be increased as a result of shorter simulation times.
- Data with high spatial and temporal resolution, see bullet above, is essential to provide the means to validate and calibrate model outcomes when one desires to implement a turbulence model into the numerical framework. With the implementation of a turbulence model, a recalibration of the Darcy-Forcheimer resistance coefficients is needed, as now they have been determined from field measurement and thus intrinsically account for turbulence within the porous media. As many turbulence closure models exist, a detailed study has to be conducted what turbulence model and what settings give the best result for wave propagation, wave breaking, porous media flow, run-up, run-down, amongst many. According to literature, this appears to be complex.
- The cobble layer in the numerical model that was used in this work was fixed. Though in reality, the rocks can move. The influence of the change in profile is approximated by averaging different the numerical overtopping discharges for the cross shore profiles measured at the start and the end of the physical experiment. The slope of the revetment is known to influence the wave breaking process and with that, overtopping discharge as well. Implementation of a sediment transport formula could help resolve this issue, as the morphological development of the cobble layer can be modelled. Not only a sediment transport formula should be added to the framework, also a modification in the source code should be made. The location of the porous media for every time step needs to be evaluated, because of the movement of the cobbles. Complexity increases even further with the consideration

that a turbulence model should be included to be able to accurately model sediment transport. It is recommended that further research should be undertaken in the following order: (i) conduct or obtain physical experimental data with high temporal and spatial resolution, (ii) implement turbulence model and simultaneously adapt mesh for proper representation of bottom friction, bottom boundary layer, return current, swash flow, porous flow, in- and ex-filtration (iii) develop sediment transport formula capable of predicting transport of only cobbles (or rock) and adapt the source code for an update of the location of the porous media in every time step, and finally, (iv) develop a sediment transport formula capable of predicting transport of sand and cobble stones simultaneously.

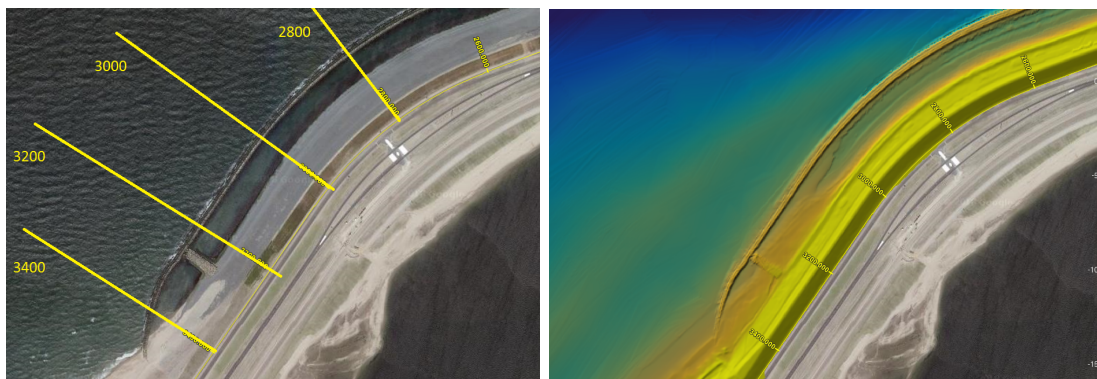
- The relative pore volume number proposed in this study was shown to have a good correlation with the overtopping from the irregular waves simulated in this study. This parameter included the influence of the spectral wave height,  $H_{m0}$ . However, as all the tests were carried out using a constant spectral wave height, the influence of  $H_{m0}$  was not investigated. Future research is suggested to investigate the performance of  $H_{m0}$ .
- The influence factor accounting for roughness,  $\gamma_f$ , was shown to have a good correlation with the relative pore volume per area. The roughness factor parameter was calculated for each experiment through rewriting the prediction formula for mean overtopping discharge on dikes and levees from EurOtop 2018. The Irribarren number, or breaker parameter,  $\xi_{m-1,0}$ , has shown to be of large influence. As all the tests presented featured a similar breaker parameter, it is suggested to investigate the influence of  $\xi_{m-1,0}$  on  $\gamma_f$ .
- The infiltration depth of water over a wave cycle into the revetment has shown to be an import parameter in quantifying the reduction of wave overtopping discharge. When the cobble layer is thicker than the infiltration depth, the extra thickness does not contribute directly in absorbing up-and-down rushing waves. However, it is also shown that the model scale experiments do not model infiltrate rate correctly, as the median cobble diameter have been scaled linearly. Future research is suggested to quantify these exact values of infiltration rate of water in to cobbles, sand and a mix of these. By following a similar analysis approach as the one presented in this study, the numerical model could be used to investigate the influence of changing the inbound wave height, period, slope of the cobble revetment, cobble diameter and crest height on the overtopping discharge on prototype scale.

# Appendix A

## Site visit

### A.1 Introduction

On Friday the 21st of September the Maasvlakte II was visited. The goal was to inspect in what sense the sand was spread on and throughout the revetment. A GPS-pack was used for positioning. Sand was collected for inspection and photos were made of the spread of sand vertically through the cobble layer. A general overview of the zone of interest including cross section marks can be found in figure A.1a. The site visit commenced at the 3400 m mark in the south-west of the revetment, after which we proceeded in a north-easterly direction down to the 2800m cross section line. There, and to the north east virtually no sand was found on or within the revetment. At 9 locations sand samples have been taken from excavated parts of the revetment, as well as photos. On cross sections of interest measurements were taken at the bottom, middle part and near the crest of the revetment such to map the cross shore spread of sand on each of the sections. In the following part footage and a thorough description can be found.



(a) Overview of the revetment. This photo is taken in Dec 2015, at that time almost no sand was yet transported to the revetment.

(b) A overview of the elevation of the seafloor, blockdam and revetment of the south west corner of the coastal barrier.

## A.2 Observations

### A.2.1 Cross shore mark 3250m

#### Bottom

A thick layer of sand lays on top of the cobbles. No cobbles are protruding through the sand layer over at least 30m in cross shore or along shore direction, see fig. A.2 for a zoomed in shot.



Figure A.2: Bottom of the revetment at cross shore mark 3250m

#### Middle

A berm is formed here and its quite steep. Sand-partially covers the cobbles, but when digging through the top layer some empty pores are found. About 90% of the area was covered with sand. See fig. A.3a and A.3b for an overview and close-up of the location where the least amount of sand was found.

#### Top

Cobbles protruding out of the sand layer, but sand has completely filled the pores. Virtually no empty pores could be detected, even when digging down by removing stones up to about 30 cm deep. It was very hard to remove the sand, it felt compacted. See fig. A.4.

### A.2.2 Cross shore mark 2950m

#### Bottom

The first location where cobbles are significantly visible through the sand layer, walking from position 3250 in north-easterly direction. No empty pores are observed. Figure A.5a shows a close up with a hole dug next to it, where as figure A.5b provides an overview. Figure A.6a gives an overview of the situation when looking in a north-easterly direction, and figure A.6b in a south-westerly direction.



Figure A.3: Middle of the revetment at cross shore mark 3250m



Figure A.4: Top of the revetment at cross shore mark 3250m

### Middle

Again a berm is found around this elevation of the revetment. Most likely formed as a result of wave impact during the high tide mark. A significant amount of sand is observed in the pores. At the foot of the steep berm there is approximately the pores are approximately for 50 % filled with sand, see fig. A.7a and A.7b for a close-up. Higher in this steep part of berm the amount of sand decreases. Figure A.8 gives an overview of the situation on the middle part of the revetment when looking into a south-easterly direction.

### Top

Not any sand, except for a few grains, can be found on the cobbles or in the pores on this part of the revetment, see fig. A.9.



(a)



(b)

Figure A.5: Bottom of the revetment at cross shore mark 2950m



(a)



(b)

Figure A.6: Bottom of the revetment looking into northerly, respectively southerly direction at cross shore mark 2950m



(a)



(b)

Figure A.7: Middle of the revetment at cross shore mark 2950m



Figure A.8: Middle of the revetment looking into southerly direction at cross shore mark 2950m



Figure A.9: Top of the revetment at cross shore mark 2950m

### A.2.3 Cross shore mark 2850m

#### Bottom

Very very small amount of sand can be found on or in the cobbles around the mid-tide mark. Plenty of sand below the mid-tide water level, e.g. the sandbank between the block dam further offshore and the mid tide mark on the revetment. See fig. A.10a for a close up and fig. A.10b for an overview in south-westerly direction.



Figure A.10: Bottom of the revetment at cross shore mark 2850m

#### Middle

No significant amount of sand can be found on the middle steep part of the cross shore section 2850m, see fig. A.11. Not any clogging, filled pores, nor sand on top of the cobbles. Just a few superficial sand grains can be observed.



Figure A.11: Middle of the revetment at cross shore mark 2850m

## Top

Plenty of sand in the pores and on the cobbles. Its a strip of sand laying in proximity of the fence of the carriageway on the top of the revetment, see fig A.12b. The sand feels light and dry. It is suspected it has been deposited there as a result of aeolian processes. An attempt has been made to dig out the cobbles and sand to find out whether the sand has completely filled the pores of the cobble revetment until the bottom, or whether it just layer in the top part. However, with no suitable equipment available, it was impossible to dig deep enough to find the answer, see fig. A.12a.



Figure A.12: Top of the revetment at cross shore mark 2850m

## A.3 Concluding remarks

It is observed that the spread of sand is irregular, inconsistent and as a result very hard to quantify. The sand could be on top of the cobble layer, with very open pores at the bottom of the structure, however, the opposite could also be possible.

Judging from the water levels and the level of the revetment it seems logical to conclude that the sand plate on the lower part of the revetment has been formed as a result of deposition by transport by sea water under the forcing of wind, waves and tidal currents. As water is powerful in forcing the grains down into the revetment it intuitively feels that the pores are quickly completely filled with sand over the whole revetment. Mathijs Mann is currently conducting research and is looking in to these processes.

On the top part of the revetment the characteristics of the sand and the shear elevation suggest that aeolian processes are dominant in depositing the sand. Here, it is harder to assume that the sand has already filled the cobble pores over the whole vertical thickness of the revetment. Again, these are all just impressions and not, in any sense, hard conclusions. With suitable equipment, excavator, GPS location stick and sediment measurements and a suitable and consistent 'grid' of sample locations in cross shore and along shore direction it is possible to find answers to these questions.

# Appendix B

## Mesh Study

The mesh is the key of the gateway to correct numerical results. Here the design is explained, then the quality of the meshes is assessed based on (i) rate of convergence, (ii) solution precision and (iii) CPU time required. This is done for two zones of interest: (a) the start of the domain just next the relaxation zone until the toe of the revetment for wave propagation processes, and (b) the top half of the revetment where wave breaking as well as wave overtopping occurs.

### B.1 The design

The layout and design of the mesh should be such that it can numerically describe the physical processes well. For a propagating 'flat' swell wave the rectangular grid can be elongated in the x-direction, i.e. the length of the cell is larger in x-direction than it is in y-direction. When waves become more steep or wave breaking occurs the cell needs to have a more square shape to capture all the details, i.e. the length of the cell in x and y direction are equal. The ratio between the length of the cell in x and y direction is called the aspect ratio. A gradual decrease of cell size in x direction is found from left to right, with the smallest cells just in front of the top of the revetment and after the top of the revetment.

The cell sizes in y direction are designed in a similar fashion. The highest level of detail is required at the water surface and no important information exists at the top and bottom boundary of the domain. The cells are elongated in y direction near the boundaries and compressed near the surface of the water. The manipulation of the cell sizes through the domain means that with less computational cells a more suitable grid can be obtained.

Wave breaking and overtopping requires a fine grid to be able to reproduce the steepness of the waves, the flow of the water within the cobbles, the overturning wave tops, the overtopping tongue, amongst many other things. Two strategies have been used for optimising performance while keeping the amount of active cells as low as possible. The first strategy has been explained in the alinea above; the gradual decrease of grid sizes to the zones of interest, and gradual increase outside the zone of interest. The second strategy is to make local refinements, see fig. B.1. The top of the revetment is refined. There the overtopping lens washes over the revetment and is small in relation to the wave. Also, the cobble layer on top of the sand core is refined so that the flow within the porous layer can be properly simulated.

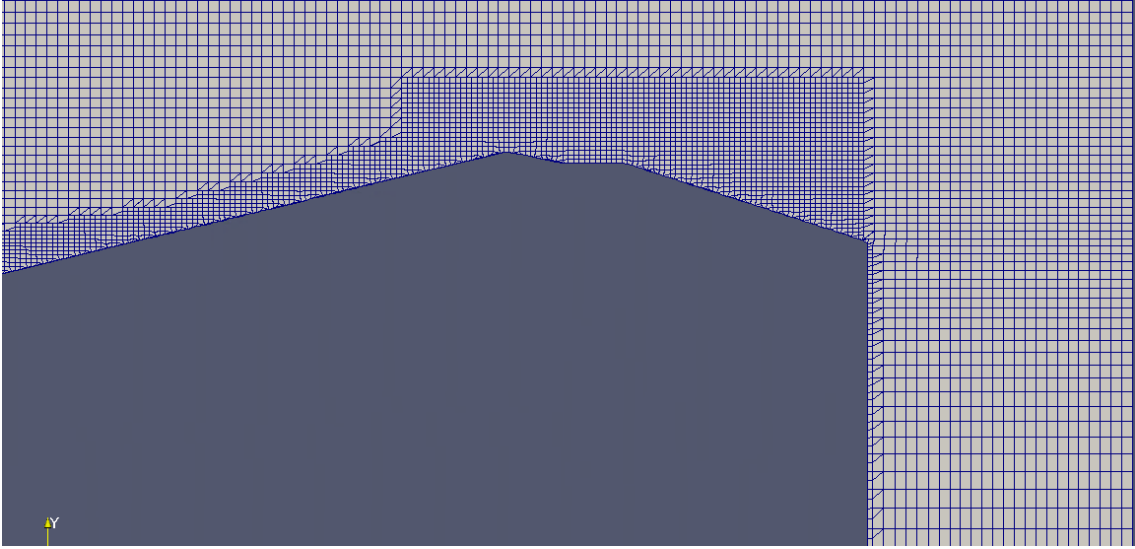


Figure B.1: A screen grab of the refinement on the top of the revetment and the sand core. This refinement enables measurements of the relatively thin layer of water that exist during overtopping events.

## B.2 Wave propagation

In figure B.2 the surface elevation over time measurements of two wave gauges of the different meshes are plotted. In table B.1 an overview is given of the properties of the meshes tested.

case ID	$N_x$	$N_y$	# cells	$\frac{H_{m0}}{\Delta y_{swl}}$	$\frac{L}{\Delta x_{toe}}$	$\frac{L}{\Delta x_{crest}}$	$t_{simulation}$ [s]	$\frac{t_{clock}}{t_{simulation}}$ [min/s]
GB02	200	28	5601	6	54	135	1600	0.37
GB08	250	25	11328	7	68	169	1600	1.29
GB01	300	42	12420	9	81	203	1600	1.30
GB03	400	55	21693	11	108	271	1600	2.63
GB09	2000	280	609339	58	543	1358	25	258

Table B.1: Overview of the several mesh resolutions and their dimensionless characteristics.

The goal here is to find a suitable mesh that is capable of simulating wave propagation and wave development at a reasonable computational cost, i.e. an acceptable clock time,  $t_{clock}$  per second simulation time,  $t_{simulation}$ . Meshes with a wide spectrum of mesh resolutions are modelled. As no surface elevation over time records are available of the physical

experiments, the mesh with the finest resolution is considered to be more correct. A test that could shed more light on this phenomenon is to model a propagating Cnoidal wave over a submerged bar, such as Shen, Ng, and Zheng 2004. Time and practical constraints, such as the in-availability of a wave flume or data made this analysis unfeasible for the author.

The coarsest mesh, GB02, models flat waves well. However, at times when waves are steep it can lack the spatial resolution, see plot bottom plot at  $t_{simulation} = 23s$  in figure B.2. Only 135 cells per wavelength and 6 cells per significant wave height have a limiting effect on the VOF MULES algorithm to discretise the steep interface and capture the details. When the resolution is increased vertically and horizontally, this effect tapers off. This is inline with the expected results. The wave height over cell size, ratio in the work of Niels G. Jacobsen, M. R. v. Gent, and Wolters 2015 is 3.3 to 4.8 for flat regular waves propagating over a sand bar.

For the sake of exploring the capabilities of the model with respect to wave propagation, a simulation of 25s with a very fine mesh is completed. This simulation GB09 shows, compared to the other coarser meshed cases, a slightly higher initial wave, after that the surface elevation over time measurements show great agreement with the other simulations at the start of the wave flume at  $x=124.5m$  and also at wave gauge 4 at  $x=150m$ . Cases GB08, GB01 and GB03 all show very similar behaviour. This suggests mesh convergence, as well as grid independence for meshes GB01, GB03 and GB09 for the phenomenon of wave propagation, but again, one cannot be sure as no physical data is available to validate this. The prohibitively high computational cost of case GB09 make it, unfortunately, impossible to simulate long enough to derive any statistical parameters to compare with the lab results.

Propagation	# cells	$\frac{t_{clock}}{t_{simulation}}$ [min/s]	convergence rate	solution precision
GB02	5601	0.14	-	-
GB08	11328	0.51	0	0
GB01	12420	0.55	+	+
GB03	21693	1.28	+	+
GB09	609339	258	+	+

Table B.2: A multi criteria assessment of the quality of the mesh for the wave propagation zone, i.e. the zone from the start of the domain at  $x = 104m$  until the zone of were wave breaking almost occurs at  $x = 150m$

### B.3 Wave run-up and overtopping

Ideally, overtopping events would be compared in a temporal framework where physically tested waves and their overtopping volume would be compared with numerical waves and their overtopping. This would lead to a better understanding of how all the individual processes such as wave breaking, wave-structure interaction, wave run up as well as overtopping are numerically modelled. In this work, no overtopping data with a temporal resolution is available. So how to go about?

The best mesh is the mesh that is simulating the physical model experiments best, assuming that wave breaking, dissipation of energy, run up and propagation of the over-

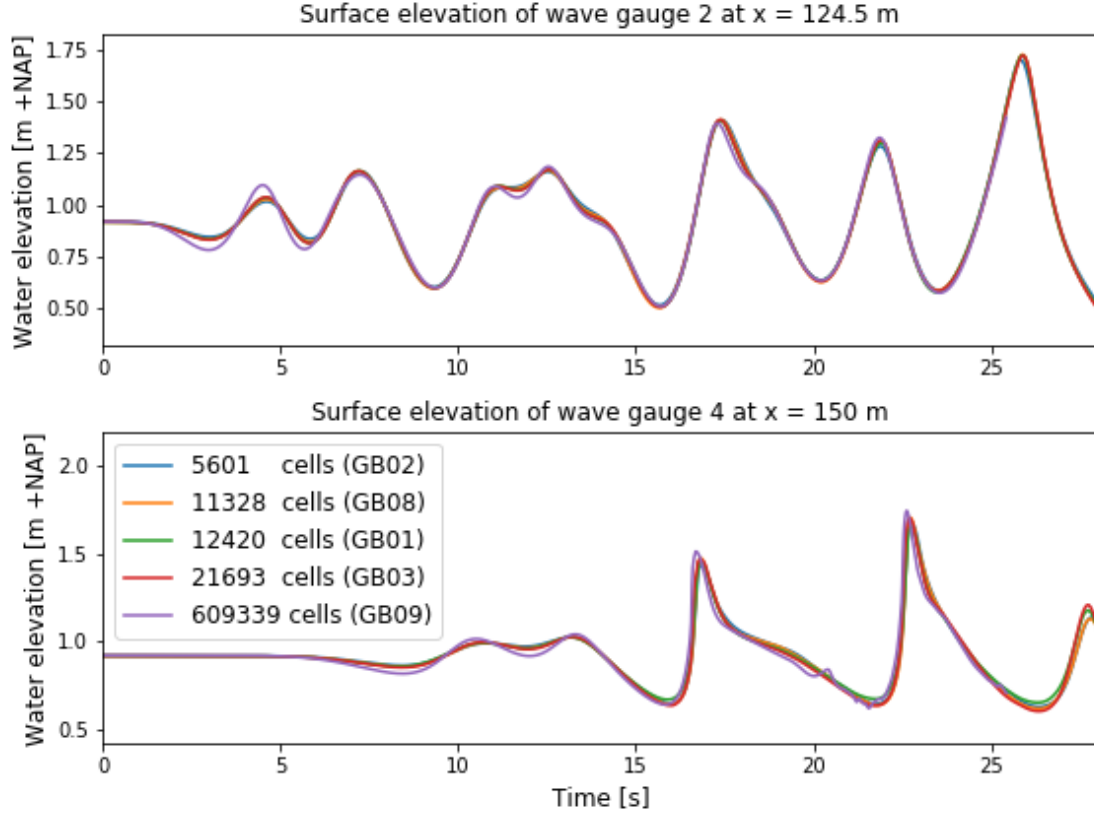


Figure B.2: Surface elevation over time measurements of wave gauge 2 at  $x = 124.5\text{m}$  and wave gauge 4 at  $x=150\text{ m}$ .

topping lens are all modelled correctly as the only data that is available is the average overtopping discharge,  $q$ , and the statistical inbound wave parameters as  $H_{m0}$ ,  $T_p$  and that the irregular waves represent a Jonswap spectrum. The goal is to find a mesh which is capable of capturing the aforementioned processes, while still computationally efficient enough such that simulation duration of at least  $t_{simulation} = 1600\text{ s}$  can be completed within  $t_{clock} = 48\text{ hours}$ . The trade-off here is computational efficiency versus accuracy. See figure B.3 for simulations with different mesh options. The way overtopping is measured numerically is stated in section 4.2.5, the lay-out of the revetment and it's setup is noted in section 4.5.2.

The case with the lowest resolution, GB02, is not able to simulate or capture the overtopping events properly. Case GB08 with 11328 active cells does capture overtopping events, however poorly. Cases with an increased resolution GB01 and GB03 capture the processes well and suggest a level of convergence. The cell resolution at the refinement of the mesh in case GB01 is  $\Delta x = 86\text{ mm}$  and  $\Delta y = 81\text{ mm}$ , and for the GB03 case  $\Delta x = 64\text{ mm}$  and  $\Delta y = 63\text{ mm}$ .

The reason why the cases with low resolutions meshes, such as GB02 or GB08, don't capture the overtopping well, can be explained by the way that overtopping is measured (see section 4.2.5). Recall that a combination of the fluid flux across a face,  $\phi$ , and the fluid flux across a face multiplied with the indicator function  $\phi_F$  is needed to evaluate the total flux across a face. However,  $\phi_F$  is not available throughout the whole time step. Therefore, in the solution to the advection equation of the indicator function the relationship in eq. 4.8 is used to estimate  $\phi_F$  with the use of  $\phi$  and  $\phi_\rho$ . As the grid size increases, more water

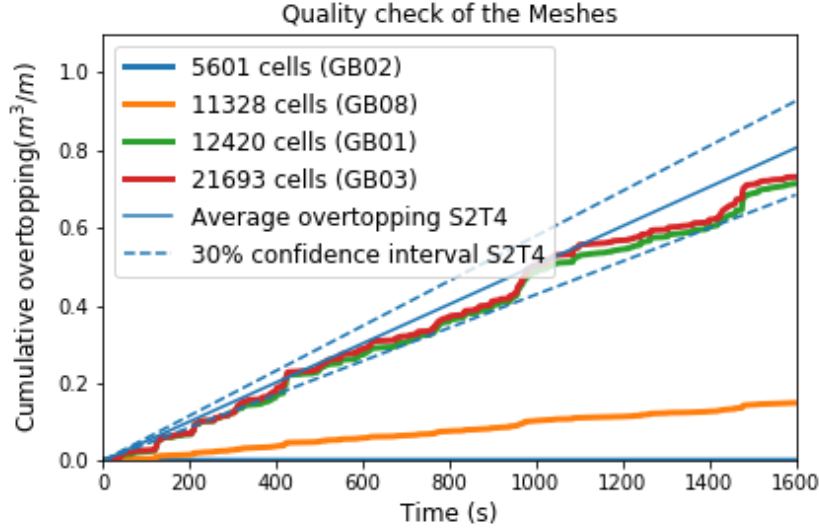


Figure B.3: Cumulative overtopping over time measurements for 4 simulations with different mesh resolutions. The mesh with the lowest resolution is not able to capture the overtopping events properly. Case GB08 with 11328 active cells does capture the overtopping lens, however poorly. Cases with an increased resolution GB01 and GB03 capture the processes well and converge.

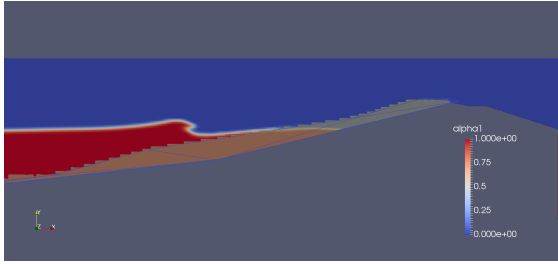
is needed to be able to fill up a cell. Now the value of  $\phi$  and  $\phi_\rho$  is less accurate and with that decreases the accuracy of the estimate of  $\phi_F$  as well. This is an explanation for the underestimation of overtopping with coarse meshes for thin overtopping films.

Overtopping	# cells	$\frac{t_{clock}}{t_{simulation}}$ [min/s]	convergence rate	solution precision	grid independence
GB02	5601	0.14	–	–	0
GB08	11328	0.51	0	0	+
GB01	12420	0.55	+	+	+
GB03	21693	1.28	+	++	+

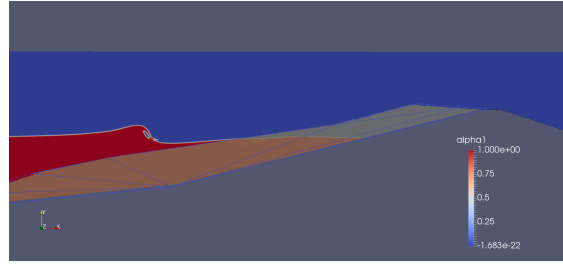
Table B.3: A multi criteria assessment of the quality of the meshes for physical processes of run up and overtopping. A much higher mesh resolution is required to model these processes of interest correctly, i.e. the steep and overturning waves, the thin water layer during overtopping and flow in the porous cobble layer.

The case with the highest resolution, GB09 is visually tested for overtopping. No lessons can be learned from it, however, as it is not a fair comparison since the profile of the GB09 is different than the GB01 and GB03 cases. The sand level is different, and with that the cobble layer thickness as well. Visual inspection does show striking similarities in the shape of the wave and the surface tracking of the VoF algorithm, see figure B.4a and B.4b for a screen shot of the simulation at  $t_{simulation} = 17$  s for case GB09 and GB03.

The



(a) Screen shot of wave break event in case GB03 at  $t_{simulation} = 17$  s



(b) Screen shot of wave break event in case GB09 at  $t_{simulation} = 17$  s

Figure B.4: A visual comparison of the same wave breaking event calculated by two different mesh resolutions.

## B.4 Conclusion

GB01, as can be seen in table B.2 and B.3, is a suitable mesh for cases where consistent overtopping is expected and is the mesh which is used for all the simulations in this work, except for cases VS13 and VS14. A higher resolution, such as simulation GB03, comes at almost three times the computational cost, but approximates the solution just slightly better. This mesh is therefore used in the VS13 and VS14 simulations aiming to reproduce the overtopping discharge as measured in the physical experiment, see section 4.5. In simulations where overtopping events are expected to be scarce and volumes are relatively low, it is better capable of capturing the small quantities of water topping over as the estimation of the fluid flux across a face multiplied with the indicator function is more precise.

# Bibliography

- Andersen, T. Lykke and H. F. Burcharth (2004). “Crest Level Assessment of Coastal Structures by Full-Scale Monitoring, Neural Network Prediction and Hazard Analysis On Permissible Wave Overtopping - CLASH”. In:
- Arana, Alejandro Hammeken (2017). “Wave run-up on beaches and coastal structures”. In: March. URL: [http://discovery.ucl.ac.uk/1546372/1/PhD\\_Thesis\\_approved\\_final\\_version.pdf](http://discovery.ucl.ac.uk/1546372/1/PhD_Thesis_approved_final_version.pdf).
- Berberović, Edin et al. (2009). “Drop impact onto a liquid layer of finite thickness: Dynamics of the cavity evolution”. In: *Phys. Rev. E* 79.3, p. 36306. DOI: 10.1103/PhysRevE.79.036306. URL: <https://link.aps.org/doi/10.1103/PhysRevE.79.036306>.
- Brown, Scott Andrew (2017). “Numerical modelling of turbulence and sediment concentrations under breaking waves using OpenFOAM®”. In: February.
- Engsig-Karup, A. P., H. B. Bingham, and O. Lindberg (2009). “An efficient flexible-order model for 3D nonlinear water waves”. In: *Journal of Computational Physics* 228.6, pp. 2100–2118. DOI: 10.1016/j.jcp.2008.11.028.
- Gent, M.R.A. van (1995). *Wave Interaction with Berm Breakwaters*. DOI: 10.1061/(ASCE)0733-950X(1995)121:5(229).
- (2009). “Dynamic Cobble Beaches As Sea Defence”. In: *Proceedings on the Third International Conference on the Application of Physical Modelling to Port and Coastal Protection* 1, pp. 1–10.
- Higuera, Pablo, Javier L. Lara, and Inigo J. Losada (2013). “Simulating coastal engineering processes with OpenFOAM®”. In: *Coastal Engineering*. ISSN: 03783839. DOI: 10.1016/j.coastaleng.2012.06.002.
- Jacobsen, Niels G., David R. Fuhrman, and Jørgen Fredsøe (2012). “A wave generation toolbox for the open-source CFD library: OpenFoam®”. In: *International Journal for Numerical Methods in Fluids* 70.9, pp. 1073–1088. ISSN: 02712091. DOI: 10.1002/flid.2726.
- Jacobsen, Niels G., Marcel R.A. van Gent, and Jørgen Fredsøe (2017). “Numerical modelling of the erosion and deposition of sand inside a filter layer”. In: *Coastal Engineering*. ISSN: 03783839. DOI: 10.1016/j.coastaleng.2016.09.003.
- Jacobsen, Niels G., Marcel R.A. van Gent, and Guido Wolters (2015). “Numerical analysis of the interaction of irregular waves with two dimensional permeable coastal structures”. In: *Coastal Engineering*. ISSN: 03783839. DOI: 10.1016/j.coastaleng.2015.05.004.
- Jacobsen, Niels Gjøøl (2017). *waves2Foam Manual*. Tech. rep. August. URL: [https://www.researchgate.net/profile/Niels\\_Jacobsen3/publication/319160515\\_waves2Foam\\_Manual/links/5995c1e7aca27283b11b21a2/waves2Foam-Manual.pdf](https://www.researchgate.net/profile/Niels_Jacobsen3/publication/319160515_waves2Foam_Manual/links/5995c1e7aca27283b11b21a2/waves2Foam-Manual.pdf).
- Jacobsen, Niels G et al. (2018). “Numerical prediction of integrated wave loads on crest walls on top of rubble mound structures”. In: DOI: 10.1016/j.coastaleng.2018.10.004. URL: <https://doi.org/10.1016/j.coastaleng.2018.10.004>.

- Jensen, Bjarne, Niels Gjøel Jacobsen, and Erik Damgaard Christensen (2014). “Investigations on the porous media equations and resistance coefficients for coastal structures”. In: *Coastal Engineering*. ISSN: 03783839. DOI: 10.1016/j.coastaleng.2013.11.004.
- Loman, G.J.A., M.R.A. Van Gent, and J.W. Markvoort (2010). “Physical model testing of an innovative cobble shore, part i: verification of cross-shore profile deformation”. In: 1, pp. 1–10.
- López De San Román Blanco, Belén (2003). “Dynamics of gravel and mixed, sand and gravel, beaches”. In: *López de San Román Blanco May*.
- Losada, Inigo J et al. (2016). “Modeling the Interaction of Water Waves with Porous Coastal Structures”. In: *The mathematical modeling of the interaction of water waves with porous coastal structures has continuously been among the most relevant challenges in coastal engineering research and practice. Finding a tool to better predict essential processes, relevan*. DOI: 10.1061/(ASCE)WW.1943-5460.0000361.
- Mann, Matthijs (2019). “Morphological sand layer dynamics: Case study at flood defence Maasvlakte 2”. In:
- Paulsen, Bo Terp, Henrik Bredmose, and Harry B. Bingham (2014). “An efficient domain decomposition strategy for wave loads on surface piercing circular cylinders”. In: *Coastal Engineering*. ISSN: 03783839. DOI: 10.1016/j.coastaleng.2014.01.006.
- Pedrozo-Acuña, Adrián et al. (2007). “A numerical-empirical approach for evaluating morphodynamic processes on gravel and mixed sand-gravel beaches”. In: *Marine Geology*. ISSN: 00253227. DOI: 10.1016/j.margeo.2007.02.013.
- She, Kaiming, Diane Horn, and Paul Canning (2007). “Influence of permeability on the performance of shingle and mixed beaches”. In: p. 105.
- Shen, Y. M., C. O. Ng, and Y. H. Zheng (2004). “Simulation of wave propagation over a submerged bar using the VOF method with a two-equation k- $\epsilon$  turbulence modeling”. In: *Ocean Engineering*. ISSN: 00298018. DOI: 10.1016/S0029-8018(03)00111-2.
- Sigurdarson, Sigurdur and Jentsje W. Van der Meer (2011). “Wave overtopping on berm breakwaters in line with Eur0Top”. In: pp. 1–15.
- Sørensen, O. R., H. A. Schäffer, and P. A. Madsen (1998). “Surf zone dynamics simulated by a Boussinesq type model. III. Wave-induced horizontal nearshore circulations”. In: *Coastal Engineering* 33.2-3, pp. 155–176. ISSN: 03783839. DOI: 10.1016/S0378-3839(98)00007-6.
- Steeg, Paul V A N, Mark Klein Breteler, and Y V O Provoost (2016). “Large-Scale physical model Tests to determine the influence of roughness for wave run-up of channel shaped block revetments”. In: pp. 1–10.
- Van der Meer, Jentsje W. et al. (2018). *EurOtop Manual*. Tech. rep.
- Vanneste, Dieter and Peter Troch (2015). “2D numerical simulation of large-scale physical model tests of wave interaction with a rubble-mound breakwater”. In: *Coastal Engineering* 103, pp. 22–41. ISSN: 03783839. DOI: 10.1016/j.coastaleng.2015.05.008.